I.J. Image, Graphics and Signal Processing, **2024, 5, 36-61**
Published Online on October 8, 2024 by MECS Press (http://www.mecs-press.org/)
DOI: 10.5815/ijigsp.2024.05.04

Modified Kalman Filter with Chebyshev Points Based on a Recurrent Neural Network for Automatic Control System Measuring Channels Diagnosing and Parring off Failures

Serhii Vladov
Kremenchuk Flight College of Kharkiv National University of Internal Affairs, Kremenchuk, 39605, Ukraine
E-mail: serhii.vladov@univd.edu.ua
ORCID iD: https://orcid.org/0000-0001-8009-5254

Oleksandr Muzychuk
Kharkiv National University of Internal Affairs, Kharkiv, 61080, Ukraine
E-mail: o.muzychuk23@gmail.com
ORCID iD: https://orcid.org/0000-0001-8367-2504

Victoria Vysotska
Lviv Polytechnic National University, Lviv, 79013, Ukraine
E-mail: Victoria.A.Vysotska@lpnu.ua
ORCID iD: https://orcid.org/0000-0001-6417-3689

Alexey Yurko
Kremenchuk Mykhailo Ostrohradskyi National University, Kremenchuk, 39600, Ukraine
E-mail: yurkoalexe@gmail.com
ORCID iD: https://orcid.org/0000-0002-8244-2376

Dmytro Uhryn*
Yuriy Fedkovych Chernivtsi National University, Chernivtsi, 58012, Ukraine
E-mail: d.ugryn@chnu.edu.ua
ORCID iD: https://orcid.org/0000-0003-4858-4511
*Corresponding Author

Received: 26 April, 2024; Revised: 28 May, 2024; Accepted: 11 July, 2024; Published: 08 October, 2024

Abstract: The article is devoted to the modified multidimensional Kalman filter with Chebyshev points development to solve the task of diagnosing and parring off failures in the measurement channels of complex dynamic objects automatic control system, which will provide a more accurate and reliable assessment of system state in the presence of outliers in the data. An implementation of the proposed modified multidimensional Kalman filter with Chebyshev points is proposed in the form of a modified recurrent neural network containing a failure diagnostics layer, a failure parry layer, a filtering and smoothing layer, and a results aggregation layer. This structure of the modified recurrent neural network made it possible to solve the main problems of the method of diagnosing and parring off failures of the measuring channels of complex dynamic objects automatic control system, such as diagnosing failures with an accuracy of 0.99802, fending off failures with an accuracy of 0.99796, and assessing the state of the system with an accuracy of 0.99798. It is proposed to use a modified loss function of a recurrent neural network as a general loss function for diagnostics, fault restoring and system state assessment, which makes it possible to avoid retraining when there are a large number of parameters or insufficient data. It has been experimentally proven that the loss function remains stable on both the training and validation data sets for 1000 training epochs and does not go beyond –2.5 % to +2.5 %, which indicates a low-risk overtraining or undertraining of the model. It has been experimentally confirmed that the use of a modified recurrent neural network in solving the task of diagnosing and parring off failures of the measuring channels of complex dynamic objects automatic control system is appropriate in comparison with a radial basis functions neural network and a multidimensional Kalman filter without a neural network implementation, based on metrics such as the root mean square deviation, mean absolute error, mean absolute percentage error, coefficient of determination for the accuracy of reproducing previous data, and coefficient of determination for the accuracy of predicting future values. For example, the value of the standard deviation of the modified recurrent neural network is 0.00226, which is 1.65 times less than the radial basis function neural network and 2.20 times less than the multidimensional Kalman filter without a neural network implementation.

Index Terms: Kalman filter, recurrent neural network, diagnosing and parring failures, automatic control system

1. Introduction

Currently, the Kalman filter is an efficient recursive filter, which, based on incomplete measurements and several noisy, allows one to estimate a dynamic system's internal state and is used in a wide range of technical devices, from car speedometers to radios and radars [1]. A typical task for the Kalman filter is to estimate past, current, or future values of position, velocity, or acceleration of some dynamic system for which its linear or instantaneously linearized model is known [2, 3].

In [4], the utilization of absolute and relative measurement data for multi-objective joint positioning was investigated, leading to the proposal of an enhanced robust distributed Kalman filter, which is divided into two stages. First, absolute measurement data are processed using a standard Kalman filter, followed by relative measurement data processed through a robust Kalman filter based on the Student's t-distribution. This approach yields more precise estimates, showing enhanced stability and positioning accuracy in environments affected by both Gaussian and non-Gaussian heavy-tailed noise. However, parameter uncertainty and limited modelling accuracy may reduce the effectiveness of the method proposed in [4] under challenging operational conditions.

In [5], several inverse Kalman filtering tasks were solved, including restoring unknown parameters and input data using posterior estimates, considering noisy or incomplete observations. The link between identifiability and solvability for inverse Kalman filtering and linear quadratic control was explored, and algorithms were proposed to estimate uncertainty covariance matrices and recover unknown sensor data. Numerical simulations validated these methods. However, noise and model uncertainty reduce estimate accuracy, impacting algorithm performance in real-world scenarios. In [6], simultaneous input and state estimation for linear discrete systems with end-to-end connections was examined, showing a transition from standard Kalman filtering to a combined estimator for unknown inputs as their variance increases. This method connects Kalman filtering with input-state estimation for systems without direct communication. However, its assumption of linearity and Gaussian noise limits real-world applicability. In [7], a filtering algorithm combining a quaternion-based extended Kalman filter with an adaptive coefficient and smooth variable structure filter was introduced for spacecraft orientation estimation, handling gyroscope drift and installation errors. The adaptive factor improves reliability while sliding mode theory reduces the impact of fast maneuvers. The drawback is the computational complexity, limiting real-time use.

Kalman filter modifications are being applied in dynamic control systems [8–10] and space tracking [11, 12], enhancing estimation and prediction efficiency. However, the lack of neural networks limits adaptive Kalman filter capabilities for managing nonlinearities and dynamic changes. Neural networks combined with Kalman filtering offer strong performance, matching second-order batch methods like Levenberg-Marquardt [13] and Quasi-Newton [14], while supporting online training for large datasets. Modifications like multi-stream learning [15] reduce local minima risks, and decoupled Kalman filters [17] save computational resources. New square root [18] and cubature Kalman filters [19] improve convergence but increase complexity. Despite advantages, neural network training via Kalman filtering faces challenges. Online training may not handle large datasets optimally, and modifications like batch training increase computational costs. For example, [20] examined state estimation for linear systems with non-Gaussian noise, using a Gaussian mixture model. Kalman innovation dynamically adapts to submodels, improving estimation. However, this approach increases the computational load in changing conditions.

In [21–24], the task of diagnosing and parring failures in the measurement channels of helicopter turboshaft engines (TE) automatic control system (ACS) is solved by developing a fault-tolerant filtering unit using a multidimensional Kalman filter, while in [21] it is proposed to train a neural network of radial-basis functions using the multidimensional Kalman filter method. The research carried out in [21–24] is based on the application of a linear adaptive on-board engine model described in [25–27]. The solution to this task is based on the use of a linear adaptive on-board engine model, which may limit the applicability of the method to complex and nonlinear systems. Although it is proposed to train a neural network of radial basis functions using the multidimensional Kalman filter method, communication with a linear model can lead to undertraining or incomplete consideration of nonlinear effects, which can reduce the efficiency of the system for diagnosing and fending off failures in real operating conditions.

Further research in this area may include a more in-depth analysis of nonlinear effects in the operation of helicopter gas turbine control systems [28, 29], as well as the development of improved models that can take into account more complex dynamic relations between system components. Research is also possible aimed at adapting neural network training methods to nonlinear engine models to improve diagnostic accuracy and prevent failures. Disadvantages associated with using a linear model can result in an inability to capture complex nonlinear effects, which can potentially limit the effectiveness of fault diagnosis and management techniques in real-world operating conditions.

The primary limitation requiring modification of the Kalman filter is its reduced accuracy and adaptability in handling nonlinearity, noise, and dynamic changes in real-world systems. Standard Kalman filters assume linear models and Gaussian noise, leading to suboptimal performance when these conditions are violated, particularly in systems with complex, time-varying dynamics or non-Gaussian disturbances. This limitation calls for advanced modifications, such as incorporating Chebyshev points to improve numerical stability and convergence in nonlinear state estimations. By leveraging Chebyshev's points, algorithms like the cubature Kalman filter can achieve higher precision in approximating integrals, thus enhancing the filter's robustness and accuracy in scenarios where traditional Kalman filtering falls short.

The work aims to improve the method for diagnosing and fending off failures in the measurement channels of helicopters' TE ACS in a fault-tolerant filtering unit using a modified multidimensional Kalman filter, which takes into account the complex dynamic relations between the helicopters' TE ACS components. The research focuses on enhancing the Kalman filter and its neural network-based modifications to improve accuracy and adaptability in dynamic systems under nonlinear conditions, noisy measurements, and uncertain model parameters.

The work scientific novelty of the results obtained lies in the improvement of the method for diagnosing and fending off failures of the measuring channels of the automatic control system of complex dynamic objects, which differs from existing ones in that, through the use of a multidimensional Kalman filter with Chebyshev points, implemented by a modified recurrent neural network, it made it possible to detect and localize sensor failures with high accuracy.

2. Material and Methods

The hypothesis requiring modification to the Kalman filter and the use of Chebyshev points suggests that the accuracy and reliability of fault detection and control sensors can be significantly improved by enhancing the filter's ability to handle nonlinearities and noise in measurement channels. Specifically, integrating Chebyshev points into the Kalman filter algorithm will improve its numerical stability and convergence when predicting piston movement in the metering needle channel, enabling more precise estimation of parameters under noisy and fault-prone conditions.

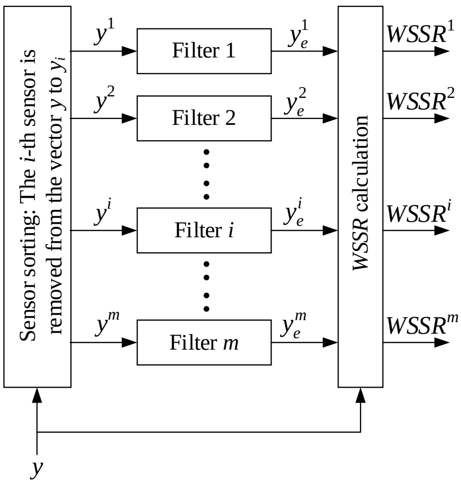

Fig. 1. The proposed polymorphic RBF network (author's research)

As mentioned above, the TV3-117 TE, which belongs to the class of helicopters TE, was chosen as the object of research in this work, due to its strategic importance for aviation safety and efficiency, which requires constant improvement and optimization of technical solutions. As described in [21–27], one of the approaches to solving the task of detecting and controlling failures in a helicopter's TE parameter sensors registered on board is the use of multidimensional Kalman filtering algorithms with a built-in system for detecting and localizing faults in the measuring channels. The mathematical model of the engine includes a fault-tolerant Kalman filter unit with a model of the dosing needle channel. This block uses the calculated value of the thermogas-dynamic parameter of helicopter TE and the predicted position of the metering needle piston (x_{given}) from helicopter TE-modified closed on-board ACS neural network. The output information of the dosing needle model is fed to the input of the differential valve model, where it is converted into a signal of the helicopter's TE thermogas-dynamic parameter. A recursive Kalman filter is connected to the output of the dosing needle model to correct the values under noisy conditions. The Kalman coefficient is adjusted in real-time to optimally estimate the piston movement. Since the measured value is used to obtain an optimal estimate, it is important to reliably detect and locate faulty measurement channels. To achieve this goal, additional logic is included in the Kalman filtering algorithms with banks of Kalman filters [22, 23] (fig. 1) to assess the measurement accuracy of a group of sensors, allowing to generate a deviation vector:

$$\boldsymbol{\varepsilon}^i = \mathbf{x}^i_{opt} - \mathbf{z}^i_{mv}, \tag{1}$$

where for the i-sensor: ε_i is the estimation error, $\mathbf{x}^i_{opt}$ is the optimal estimate (at the output of the Kalman response filter), $\mathbf{z}^i_{mv}$ is the the measured value of the piston displacement.

To identify faults in sensors, a matrix of weighted sums of squared differences **WSSR** is calculated, which represents a characteristic (or indicator) of a fault [22, 23, 25, 26], using the matrix equation:

$$\mathbf{WSSR}^i = \frac{\mathbf{W}^i_r \left(\boldsymbol{\varepsilon}^i\right)^T \boldsymbol{\varepsilon}^i}{\Sigma^i}, \tag{2}$$

where matrix $\Sigma^i = diag\left[\boldsymbol{\sigma}^i\right]^2$.

The vector $\boldsymbol{\sigma}^i$ represents the standard deviation of the i-th sensor, normalizing the deviation. The matrix of weight coefficients $\mathbf{W}_r$ contains engineering settings selected in such a way that the sum of the elements of the **WSSR** matrix does not exceed a certain set value when all sensors operate properly. If the $\mathbf{W}_r$ matrix is unit and $\varepsilon^i = \sigma^i$, then the corresponding element of the **WSSR** matrix will be equal to the number of measuring channels in the group. If $\varepsilon^i \neq \sigma^i$, a simplified expression is used by [22, 23, 25, 26]:

$$WSSR = \sum \frac{\varepsilon^2}{\sigma^2}. \tag{3}$$

It is important to note that a similar expression (2) is also used for one of the channels of a two-channel sensor. To detect a failure in one of the sensor channels, its corresponding **WSSR** value is compared with a threshold value that is expertly set based on the analysis of statistical experimental data for a specific helicopter gas turbine engine. It is also important to consider that a low threshold level can cause false alarms, while a high threshold level can reduce the sensitivity of the system to failures. By [22, 23, 25, 26], it is recommended to select a failure signature value ranging from 1.5 to 2 (a threshold of 2 is selected).

The algorithm for detecting and localizing a failure of the travel sensor channel is illustrated in table 1. When integrating Kalman bank filters with neural network technologies, the modified generalized block diagram of the process of setting the parameters of the neural network model of the helicopter gas turbine engine has the form shown in fig. 2. The functionality of bank Kalman filters is given in table 2.

Table 1. Algorithm for detecting and localizing a channel failure of a two-channel sensor (author's research published in [22, 23] based on [25, 26])

$WSSR_1$	$WSSR_2$	Situation	The output is received
≤ 2	≤ 2	Both channels are OK	A filtered (Kalman) measurement of the channel with the lowest **WSSR**
≤ 2	≥ 2	Second channel failure	A filtered (Kalman) measurement of the first channel
≥ 2	≤ 2	First channel failure	A filtered (Kalman) measurement of the second channel
≥ 2	≥ 2	Both channels failed	Model value of piston displacement x_{dn}

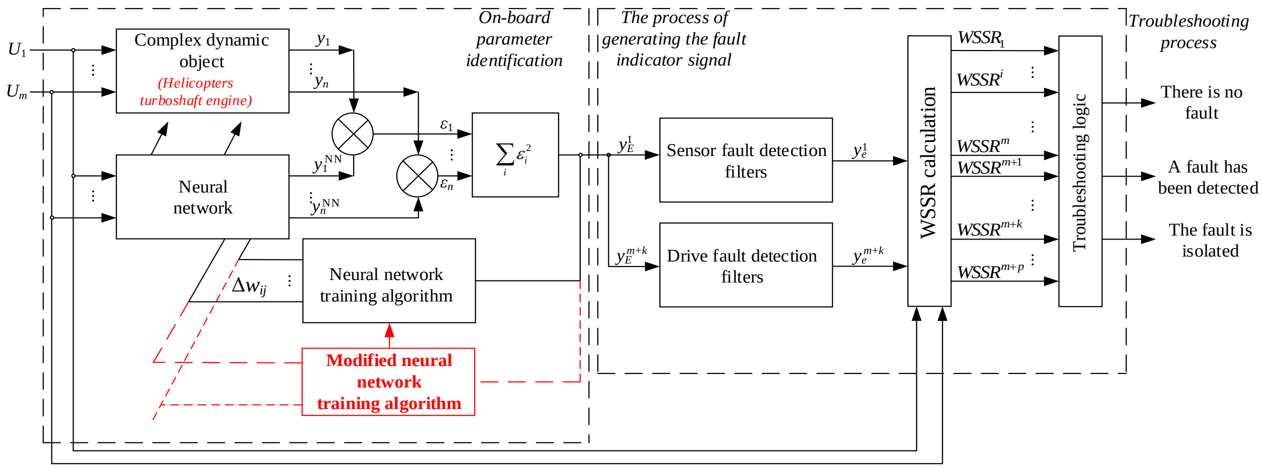

Fig. 2. A modified training diagram of the neural network model of complex dynamic objects with integrated Kalman bank filters (author's research based on [21–27])

Table 2. Algorithm for detecting and localizing a channel failure of a two-channel sensor (author's research based on [21–27])

<table>
<tr><th colspan="2">Case 1</th><th>Case 2</th></tr>
<tr><td colspan="2">With or without fault detection, Kalman filters preserve low-level indicator signals, showing the lack of correctness, and generate accurate estimates within operating limits.</td><td>When one sensor or mechanism fails, only one filter with the correct hypothesis generates a fault indicator signal and accurate parameter estimates within operating limits.</td></tr>
<tr><td>Conclusions</td><td colspan="2">1. Fault indicator signals necessitate additional processing for fault detection, which can be achieved by incorporating a set of Kalman filters alongside fault isolation algorithms.
2. Fault isolation algorithms are determined by detection thresholds and decision rules, illustrated in fig. 2. This decision-making process evaluates fault indicator signals against predefined thresholds, declaring a fault if the specified detection criteria are satisfied.
3. Fault isolation is successful when a fault is identified for all indicator signals except the one that aligns with the accurate fault hypothesis. The design of fault isolation algorithms is tailored to the specific application requirements.</td></tr>
</table>

According to [25–27, 30], an analysis of real noise from TV3-117 TE flight tests revealed that the noise characteristics include a zero mean, constant variance, and consistent spectra across both large and small samples. This supports the hypothesis of process ergodicity, as the mean and variance remain stable over time and across different implementations. The Pearson criterion verifies the normal distribution of the noise, facilitating the use of Kalman filters (and neural networks trained with Kalman filters) for this type of process [30, 31]. As noted in [30, 32], the objective is to minimize errors in both the model channel (predicted parameter values) and the measurement channel (current sensor readings) across four parameters: G_T is the fuel consumption, n_{TC} is the gas generator rotor r.p.m., n_{FT} is the free rotor turbine speed, T_G^* is the gas temperature in front of the compressor turbine [28–30, 32]. Classic multidimensional Kalman filters, discussed in [21–27], rely on computing the Kalman coefficient and correlation matrices, which are updated each cycle and provide second-order error surface information, offering advantages over first-order methods like gradient descent. This approach allowed [21] to train a radial basis function neural network using the extended Kalman filter method to handle scenarios with both operational and failed measuring channels in helicopter TE ACS. A major drawback of the classical multidimensional Kalman filter is the substantial computational resources required for the continuous calculation of these matrices [21–27]. To address these issues, [33] proposes an initial stage involving the mathematical representation of a nonlinear dynamic model of complex dynamic objects as a system of differential equations:

$$\begin{cases} \dfrac{\Delta y_1(t)}{\partial t} = a_{11} \cdot y_1(t) + a_{12} \cdot y_2(t) + \ldots + a_{1n} \cdot y_{n-1}(t) + b_{11} \cdot x_1(t) + b_{12} \cdot x_2(t) + \ldots + b_{1m} \cdot x_{m-1}(t), \\ \dfrac{\Delta y_2(t)}{\partial t} = a_{21} \cdot y_1(t) + a_{22} \cdot y_2(t) + \ldots + a_{1n} \cdot y_{n-1} + b_{21} \cdot x_1(t) + b_{22} \cdot x_2(t) + \ldots + b_{2m} \cdot x_{m-1}(t), \\ \ldots \\ \dfrac{\Delta y_n(t)}{\partial t} = a_{n1} \cdot y_1(t) + a_{n2} \cdot y_2(t) + \ldots + a_{nn} \cdot y_{n-1} + b_{31} \cdot b_{n1} \cdot x_1(t) + b_{n2} \cdot x_2(t) + \ldots + b_{nm} \cdot x_{m-1}(t), \end{cases} \tag{4}$$

A special case of which for helicopters TE has the form:

$$\begin{cases} \dfrac{\Delta \partial n_{TC}(t)}{\partial t} = a_{11} \cdot n_{TC}(t) + a_{12} \cdot n_{FT}(t) + a_{13} \cdot T_G^*(t) + b_{11} \cdot G_T(t), \\ \dfrac{\Delta \partial n_{FT}(t)}{\partial t} = a_{21} \cdot n_{TC}(t) + a_{22} \cdot n_{FT}(t) + a_{23} \cdot T_G^*(t) + b_{21} \cdot G_T(t), \\ \dfrac{\Delta \partial T_G^*(t)}{\partial t} = a_{31} \cdot n_{TC}(t) + a_{32} \cdot n_{FT}(t) + a_{33} \cdot T_G^*(t) + b_{31} \cdot G_T(t). \end{cases} \tag{5}$$

To reduce the computational complexity of the extended Kalman filter method [21–27], in this work, use an alternative method – a Kalman filter with Chebyshev points, which will avoid the need to calculate Jacobians and covariance matrices at each step, since Chebyshev points are the nodes at which the interpolation polynomial Chebyshev takes maximum values in absolute value, which are used in numerical analysis methods such as interpolation and numerical integration to reduce errors that can occur when points are distributed uniformly [34, 35].

To improve the stability and reliability of diagnostics of failures of measuring channels, as well as increase the accuracy of assessing the state of the system in the presence of failures, this work proposes a modification of the Kalman filter with Chebyshev points (table 3).

Table 3. Algorithm for detecting and localizing a channel failure of a two-channel sensor (systematized by the author)

Approach	Description
Adaptive Chebyshev point selection strategy	Development of an algorithm that dynamically adapts the location of Chebyshev points depending on system dynamics and noise characteristics, for example, by applying an optimization method to select Chebyshev points in a manner that minimizes system state estimation error.
Accounting for information on the quality of measurements	Instead of using a fixed threshold to check for failures of measurement channels, an adaptive threshold is introduced that depends on the quality of the measurements, for example, using information about the measurement dispersion to determine the failure threshold.
Using a variable structure Kalman filter (VSKF)	In the event of measurement channel failures, VSKF is enabled, which allows dynamic changes to the Kalman filter structure, including adding or removing measurement channels from the system state estimate.
Using machine learning algorithms	Machine learning algorithms such as recurrent neural networks or deep learning algorithms are used to adaptively estimate the covariance matrices of process and measurement noise.
Conclusion	The integration of these methods will significantly improve the performance of the system for diagnosing and fending off failures of measuring channels in the automatic control system of helicopter gas turbine engines, ensuring high accuracy in assessing the state of the system and a quick response to failures.

It is assumed that x is the system state vector, z is the measurement vector, F is the transition matrix for the dynamic model of the system, H is the measurement matrix, Q is the covariance matrix of process noise, and R is the covariance matrix of measurement noise.

At the first stage of the proposed method, the initial state of the system x_0, the covariance matrix P_0 and the measurement matrix H are initialized.

Next, n Chebyshev points ξ_i are selected in the interval [–1, 1] and the corresponding weights ω_i with subsequent minimization of the cost function J, taking into account the error in estimating the state of the system, by applying the optimization method.

It is assumed that the system state estimation error e_k is given, which is defined as the difference between the actual value and the estimated value of the system state:

$$e_k = x_k - x_k. \tag{6}$$

The cost function J as the sum of squared estimation errors for each Chebyshev point is determined according to the expression:

$$J = \sum_{i=1}^{n} \omega_i \cdot \left(e_k\left(\xi_i\right)\right)^2, \tag{7}$$

where ω_i is the weight corresponding to each Chebyshev point, $e_k(\xi_i)$ is the error in estimating the state of the system at the Chebyshev point ξ_i.

The optimization task (7) can be formulated as follows:

$$Z = \min_{\omega_1, \omega_2, \ldots, \omega_n} J \tag{8}$$

with restriction

$$\sum_{i=1}^{n} \omega_i = 1, \quad \omega_i \geq 0, \quad i = 1, 2, \ldots, n. \tag{9}$$

Solving the optimization task (7) with constraints (8) will allow us to find optimal weights ω_i that minimize the error in estimating the state of the system at the selected Chebyshev points. To do this, it is proposed to use an optimization algorithm based on evolutionary strategies (table 4) [36], the advantage of which over other optimization algorithms, for example, the gradient descent algorithm, is its ability to bypass local optima and work in function spaces where gradients are not defined or ineffective.

Table 4. Main stages of the optimization algorithm based on evolutionary strategies (systematized by the author based on [36])

Stage number	Stage name	Description
1	Population initialization	A population P of size N is initialized randomly, in which an individual represents a set of weights ω_i for all Chebyshev points.
2	Fitness assessment	For each individual in the population, the value of the cost function J is calculated using the current weights ω_i.

3	Parents' choice	Parent selection is performed to create new individuals using tournament selection, which provides a more efficient and robust parent selection while minimizing the impact of outliers and noise in the data compared to fitness-based proportional selection. To conduct a tournament for a population P of size N, p individuals p_1, p_2, …, p_k (where p – the size of the tournament, usually taken to be 2 or 3) are randomly selected from the population, then these individuals are compared based on a certain metric M – the fitness function. An individual for mutation M is selected by the expression: $M = \arg\max\left(f\left(p_1\right), f\left(p_2\right),..., f\left(p_k\right)\right)$. Tournament selection allows you to select an individual for mutation, taking into account its competitiveness with other randomly selected individuals from the population, since the individual that has the best value of the M metric wins.
4	Creation of offspring (reproduction)	For each pair of parents, offspring are created using mutation and crossover operators.
5	Mutation	The mutation operator is applied to the offspring by adding random noise to the weights of each individual to explore new solutions in the parameter space according to $\omega_i' = \omega_i + \delta_i$, where δ_i – random value from some distribution of the random noise vector $\mathbf{\Delta} = (\delta_1, \delta_2, \ldots, \delta_n)$ (for example, the normal distribution) with zero mean and a given standard deviation, ω_i – weight of the current individual in the offspring $\omega = (\omega_1, \omega_2, \ldots, \omega_n)$.
6	Crossover	Applies a crossover operator to the offspring by combining the weights of the parents to create new combinations according to $\omega_i'' = \begin{cases} \omega_{1,i}', \text{ if } i \le z, \\ \omega_{2,i}', \text{ if } i > z, \end{cases}$ where ω_i'' – new weight in the offspring, $\omega_{1,i}'$ and $\omega_{2,i}'$ – the corresponding weights for the first $\omega_1' = \left(\omega_{1,1}', \omega_{1,2}',..., \omega_{1,n}'\right)$ and second $\omega_2' = \left(\omega_{2,1}', \omega_{2,2}',..., \omega_{2,n}'\right)$ parent, $z \in \left(1, n-1\right)$ – random place of division.
7	Assessment of offspring fitness	For each offspring individual, the value of the cost function J is calculated.
8	Selecting survivors (selection)	The best individuals for the next generation are selected based on their fitness using elitism, which takes into account not only current rank or position but also the potential flow of innovation, diversity and unique qualities.
9	Repetition	Steps 3–8 are repeated until the stopping criterion is reached – the maximum number of generations is reached and the specified accuracy is achieved.

The next step is to update the adaptive threshold for failures by calculating the adaptive threshold T_i based on its variance σ_i^2 for each measurement channel i. To do this, the adaptive threshold T_i is set as a function of several standard deviations σ_i from the mean value. This allows thresholds to be set based on the statistical characteristics of the data, making them more adaptive to changes in the data. It is assumed that k is a coefficient that determines how many standard deviations are supposed to be used as a threshold. Then the adaptive threshold T_i for measuring channel i is calculated as:

$$T_i = k \cdot \sigma_i, \tag{10}$$

where σ_i is the standard deviation for measuring i-th channel.

After calculating the adaptive threshold, the measurement matrix H is adaptively updated by eliminating measurement channels that show signs of failure and updating the measurement matrix H by eliminating the corresponding rows. According to the conditions of the task, a measurement matrix H of dimension $m \times n$ is specified, where m is the number of measurements, and n is the number of states or state variables, and it is assumed that each measuring channel has failure indicators, designated as $fault_i$, where i is the index of the measuring channel. Let $fault_i$ = 1 mean that i-th channel is showing signs of failure. Then it is possible to create a new measurement matrix H′, excluding the rows corresponding to channels with signs of failure, that is:

$$\mathbf{H}' = \begin{pmatrix} h_1 \\ h_2 \\ ... \\ h_m \end{pmatrix}, \tag{11}$$

where h_i is the i-th row of the matrix H, corresponding to the i-th dimension, for which $fault_i$ = 0.

The updated measurement matrix H will contain only those rows that correspond to healthy measurement channels, that is, H = H′. This update ensures that only healthy measurement channels are used when updating the system state estimate using the Kalman filter.

After this, the following states of the system and the covariance matrix of the error are predicted:

$$\begin{aligned} \bar{x}_{k+1} &= F \cdot x_k, \\ P_{k+1}^- &= F \cdot P_k \cdot F^T + Q. \end{aligned} \tag{12}$$

For each *i*-th Chebyshev point, the following parameters are calculated:

- Measurement predicts:

$$\hat{z}_i = \mathbf{H} \cdot \bar{x}_{k+1}. \tag{13}$$

- Innovations:

$$y_i = z_i - \hat{z}_i. \tag{14}$$

- Kalman matrices:

$$K_i = P_{k+1}^{-} \cdot H^T \cdot \left(H \cdot P_{k+1}^{-} \cdot H^T + R\right)^{-1}. \tag{15}$$

- Adjustments to the system state predict:

$$\overset{+}{x}_{k+1} = \bar{x}_{k+1} + K_i \cdot y_i, \tag{16}$$

- Updates to the error covariance matrix:

$$P_{k+1}^{+} = P_{k+1}^{-} \cdot \left(I - K_i \cdot H\right). \tag{17}$$

At the final stage, a check for failures of the measuring channels is carried out. Each measurement is checked to see if the adaptive threshold T_i is exceeded. For each measurement *i*-th channel, it is checked whether the residual between the current measurement $z_{k,i}$ and the predicted measurement exceeds $\hat{z}_{k,i}$ the adaptive threshold T_i as:

$$\left| z_{k,i} - \hat{z}_{k,i} \right| > T_i. \tag{18}$$

If the residual (18) exceeds the threshold T_i, this means that measuring *i*-th channel shows signs of failure. If measuring *i*-th channel shows signs of failure, then it is excluded from the condition assessment. The updated matrix H will contain only those rows that correspond to serviceable measuring channels, that is, the rows corresponding to channels with signs of failure are excluded, and we form a new matrix H = H′ without these rows, where H′ is the measurement matrix without rows corresponding to the channels with signs of failure. After updating the matrix H, the necessary parameters are recalculated according to (11)–(17). This procedure is repeated until the residual (18) does not exceed the threshold T_i. Thus, the proposed method allows you to quickly respond to failures in measurement channels by excluding the corresponding channels from the state assessment and updating the measurement matrix.

The proposed method for diagnosing and countering failures of measuring channels in an automatic control system of complex dynamic objects using modifications of the Kalman filter with Chebyshev points ensures the convergence of the assessment of the system state to the true value and the stability of the system to failures of measuring channels. Convergence as a constraint on the difference between the true state and the estimated state is formulated as:

$$\lim_{k \to \infty} \left(\mathbf{x}_k - \mathbf{x}_k \right) = 0, \tag{19}$$

where $\mathbf{x}_k$ is the vector of the true state of the system at a time, and $\mathbf{x}_k$ is the state estimate obtained using modifications of the Kalman filter with Chebyshev points. Chebyshev's points are evenly distributed over the time interval and are taken into account when updating the state estimate, which provides a more accurate estimate even in the face of changing system dynamics. Also, diagnostic and fault correction mechanisms allow the system to quickly detect and compensate for failures in the measuring channels. As a result, the proposed method ensures the convergence of the system state estimate to the true value.

Since for each measuring *i*-th channel there is an adaptive threshold T_i, which determines the maximum permissible discrepancy between the current measurement $z_{k,i}$ and the predicted measurement $\hat{z}_{k,i}$, then (18) is a condition for the stability of the system to failures, which means the stability of the assessment of the system state in the presence of failures in the measuring channels, since the proposed method allows us to correctly detect and compensate for these failures.

To implement the proposed method for diagnosing and countering failures of measuring channels in the automatic control system of complex dynamic objects using modifications of the Kalman filter with Chebyshev points to increase the generalization ability of the model and resistance to various types of data and variations in the data, it is advisable to use a modified recurrent neural network (fig. 3), which has the following structure:

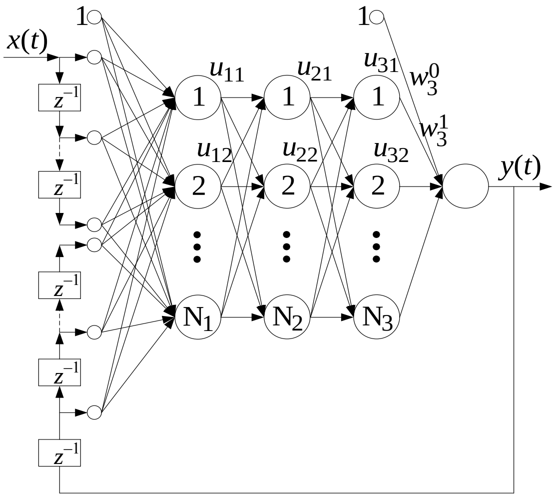

Fig. 3. Structure of a modified recurrent neural network for diagnosing and fending off failures of measuring channels in the automatic control system of complex dynamic objects (using the example of TV3-117 turboshaft engine) (author's research)

1. Failure diagnostics layer – takes as input time sequences of measurements from three measuring channels and is implemented as a recurrent layer, since it must take into account time dependencies in the data. The recurrent layer is followed by a dense layer or several dense layers to classify the probability of the presence or absence of failures in each measurement channel.

2. Failure parry layer – analyzes predictions from the fault diagnosis layer and adjusts the system state estimate when faults are detected and is implemented as a recurrent layer followed by dense layers or a combination of convolutional and recurrent layers to analyze spatial and temporal patterns in the data.

3. Filtering and smoothing layer – improves the assessment of system state, taking into account time dependencies and smoothing out noise and artefacts, and is implemented as a recurrent layer with several layers of recurrent neurons for taking into account time dependencies.

4. Results aggregation layer – accepts predictions and decisions from previous layers as input and makes the final decision on the state of the system fends off failures, and is implemented as a dense layer for combining and processing predicts.

To train the developed modified recurrent neural network for diagnosing and fending off failures of measuring channels in complex dynamic objects automatic control system, it is assumed that $X = (x_1, x_2, \ldots, x_T)$ is the given time sequences of measurements of measuring channels, where each x_t is a vector of measurements at the moment time t, $Y = (y_1, y_2, \ldots, y_T)$ is the corresponding failure marks for each measuring channel, where each y_t can take values 0 (norm) or 1 (failure). It is accepted that the proposed modified recurrent neural network consists of several layers: a failure diagnostic layer, a failure parry layer, a filtering and smoothing layer, and a results aggregation layer, and is a composition of functions of the form:

$$f(X) = A\Big[G\Big(H\big(D(X)\big)\Big)\Big], \tag{20}$$

where D is the fault diagnosis layer, H is the fault parsing layer, G is the filtering and smoothing layer, and A is the result aggregation layer.

To train the proposed modified recurrent neural network in general form, the backpropagation algorithm [37] is used, according to which it is necessary to minimize the loss function L according to the network parameters θ. According to the proposed structure of the modified recurrent neural network, the loss function consists of several components that evaluate the quality of fault diagnostics (L_{diag}) and fault parrying ($L_{correct}$), as well as an assessment of the system state (L_{state}), that is:

$$\min_{\theta} L\big(f(X), Y\big). \tag{21}$$

The loss function L is a generalized loss function for diagnosing failures (L_{diag}), for countering failures ($L_{correct}$) and for assessing the system state (L_{state}) and is determined according to the expression:

$$L_{diag} = -\frac{1}{N} \cdot \sum_{i=1}^{N} \left(y_i \cdot \log\left(y_i \right) + \left(1 - y_i\right) \cdot \log\left(1 - y_i\right) \right) + \lambda_{diag} \cdot RegTerm_1, \quad (22)$$

$$L_{correct} = -\frac{1}{N} \cdot \sum_{i=1}^{N} \left(y_i \cdot \log\left(y_i \right) + \left(1 - y_i\right) \cdot \log\left(1 - y_i\right) \right) + \lambda_{correct} \cdot RegTerm_2, \quad (23)$$

$$L_{state} = \frac{1}{N} \cdot \left\| X_i - X_i \right\|^2 + \lambda_{state} \cdot RegTerm_3, \quad (24)$$

where N is the number of examples in the training set, y_i and y_i is the corresponding labels and predicted probabilities of failures for the ***i***-th example, y_i is the predicted probabilities of parrying failures from the neural network for the ***i***-th example, X_i is the predicted values of the system state, X_i is the actual values of the system state, λ_{diag}, $\lambda_{correct}$, λ_{state} is the corresponding regularization coefficients that regulate the contribution of regularization to the overall loss function, $RegTerm_1$, $RegTerm_2$, $RegTerm_3$ are regularization terms that depend on the model parameters and its complexity.

It's worth noting that adding regularization to loss functions can help improve a model's generalization ability and reduce the risk of overfitting, especially when there is a large set of parameters or a small amount of data. Methods for selecting regularization coefficients are given in table 5.

Table 5. Basic methods for selecting regularization coefficients (systematized by the author based on [38])

Method	Description
Cross-validation method	By dividing the original data set into training and validation samples, train the model with different values of the regularization coefficient on the training set and evaluate its performance on the validation set, based on which the values of the coefficients that give the best performance on the validation set are selected.
Sliding control method	Applying the full training set, iteratively splitting it into training and validation datasets and evaluating performance for different values of the regularization coefficient.
Empirical choice	Applying rules of thumb or guidelines to select an initial value for the regularization coefficient, based on knowledge of the type of problem and size of the data.
Grid search	It consists of searching through the values of the regularization coefficient from a predefined range and choosing the one that gives the best performance on the validation set.

The regularization term usually depends on the model parameters and their complexity. One of the common regularization methods, L_1 or L_2 regularization [39], adds fines for model complexity to prevent overfitting (table 6).

Table 6. Basic methods for selecting regularization coefficients (systematized by the author based on [39])

Parameter	L_1 regularization	L_2 regularization
Description	Represents the sum of the absolute values of all model parameters.	Represents the sum of the squares of all model parameters.
Expression	$RegTerm_{L1} = \lambda \cdot \sum_{i=1}^{N} \lvert\theta_i\rvert$	$RegTerm_{L2} = \lambda \cdot \sum_{i=1}^{N} \theta_i^2$
Variables	λ – regularization coefficient, θ_i – model parameters, N – number of parameters	
Conclusion	The choice between L_1 and L_2 regularization depends on the specifics of the problem and the properties of the data. L_1 regularization can lead to sparse models, useful for feature selection, while L_2 regularization helps smooth model parameters and avoid large weights.	

In (22), α, β, γ are coefficients that take into account the relative influence of each task on the overall loss function, approaches to calculating which are described in table 7 [40].

Table 7. Basic approaches to calculating coefficients α, β, γ in (22) (systematized by the author based on [40])

Approach	Description
Expert determination	Domain experts can estimate the relative impact of each task on the overall loss function and suggest initial values for the coefficients. This approach is often used in cases where precise statistical information about the impact of each task is not available.
Cross-validation	The cross-validation method can be used to assess the quality of the model for various coefficient values. For each set of coefficient values, you can calculate the average model performance score and select those that demonstrate the best performance on the validation set.
Grid search	The grid search method can be used to systematically search through different combinations of coefficient values over a given range. For each combination of coefficient values, the model is trained and evaluated on the validation set, and those that give the best quality are selected.
Optimization by optimization method	Apply gradient descent optimization or other function optimization techniques to find optimal coefficient values directly from the training data. This approach requires the formulation of an objective function that depends on the coefficients.
Automatic machine learning	You can use automatic machine learning techniques, such as automated hyperparameter mining (AutoML), to automatically select optimal coefficient values based on a given optimization criterion.

In the proposed modified recurrent neural network training algorithm, after each training epoch, the network predictions are filtered and smoothed using the proposed Kalman filter algorithm using Chebyshev points.

After training the model, its performance is evaluated on a test data set. Quality metrics, such as the accuracy of fault diagnosis, the accuracy of fault correction, and the accuracy of system state assessment [41], are given in table 8.

Table 8. Basic quality metrics (systematized by the author)

Metric	Description	Mathematical expression
Failure diagnostic accuracy	Measures the proportion of correctly classified measurement channel failures relative to all failures.	$Accuracy_{diag} = \frac{TP}{P}$, where *TP* is the number of correctly classified failures, and *P* = *TP* + *FN* – the total number of failures.
Failure parry accuracy	Measures the proportion of successfully eliminated failures of measuring channels with all detected failures.	$Accuracy_{correct} = \frac{TN}{D}$, where *TN* is the number of successfully resolved failures, and *D* = *TP* + *FP* – is the total number of detected failures.
System state assessment accuracy	Measures the degree of accuracy in estimating the system state using a neural network. It can be a measure of the similarity between predicted and actual values of a system's state.	$R^2 = \frac{\frac{1}{N} \cdot \sum_{i=1}^{N} \left(X_i - X_i \right)^2}{\frac{1}{N} \cdot \sum_{i=1}^{N} X_i}$.

Failure diagnostic accuracy is calculated by dividing the number of correctly identified measurement channel failures by the total number of actual failures, reflecting the proportion of accurate classifications relative to all detected failures. Conversely, failure parry accuracy is determined by dividing the number of successfully mitigated measurement channel failures by the total number of detected failures, indicating the proportion of effectively managed failures among all identified failures. These metrics together assess the effectiveness of a diagnostic and fault mitigation system in identifying and addressing sensor failures. Practically, these measurements are crucial for enhancing system reliability and operational safety. High diagnostic accuracy ensures that the system can reliably identify faults, reducing the risk of undetected issues. High parry accuracy demonstrates the system's effectiveness in not only detecting but also successfully mitigating faults, thereby preventing potential failures from affecting overall system performance. Together, these metrics support the development and deployment of more robust and resilient diagnostic systems in complex engineering applications.

The results obtained allow us to formulate and prove two theorems.

Convergence theorem for the training algorithm of a modified recurrent neural network using the Kalman filter algorithm with Chebyshev points: "When using the Kalman filter algorithm with Chebyshev points to update the parameters of a modified recurrent neural network, sequentially minimizing the loss function, and also taking into account regularization to prevent overfitting of the model, the training process will converge to a locally optimal solution".

Proof:

Let a neural network be given with an architecture defined within the framework of the proposed method for diagnosing and fending off failures of measuring channels in an automatic control system for complex dynamic objects. Let also be given a training data set D and a loss function L(D, H, Θ) that evaluates the difference between model predictions and actual values.

To prove that the introduction of a Kalman filter with Chebyshev points allows one to effectively take into account noise and uncertainties in the data, which facilitates the convergence of the training process, x_t is the system state vector, z_t is the observed measurement, H_t is the measurement matrix, Q_t is the process covariance matrix, R_t is the measurement covariance matrix. The state update by the Kalman filter algorithm is expressed as:

$$\mathbf{x}_t = \mathbf{F}_t \cdot \mathbf{x}_{t-1} + \mathbf{B}_t \cdot \mathbf{u}_t + \mathbf{K}_t \cdot \left(\mathbf{z}_t - \mathbf{H}_t \cdot \mathbf{x}_t \right), \tag{25}$$

where $\mathbf{x}_t$ is the state assessment at time *t*, F_t is the state transition matrix, B_t is the control matrix, u_t is the control vector, K_t is the Kalman matrix.

State update expression (26) by the Kalman filter algorithm integrates the measurement information and the previous estimate of the system state, taking into account the process covariance and measurement covariance. State transition matrix F and control vector u are used to predict the next state of the system based on the previous state and external control. The measurement matrix H is used to map the expected measurement to the current state of the system. The Kalman matrix K, calculated from the process covariance Q and the measurement covariance R, determines how much to adjust the predicted state of the system based on the difference between the expected and actual measurement. This allows you to account for uncertainties in the data, such as measurement noise and unknown influences on the system state.

To prove that the use of regularization allows you to control the complexity of the model and prevent its overfitting, which contributes to more stable convergence, a regularization is introduced to control the complexity of the model of the form:

$$\mathbf{L}_{reg}(\mathbf{\Theta}) = \mathbf{L}(\mathbf{D}, \mathbf{H}, \mathbf{\Theta}) + \boldsymbol{\lambda} \cdot \mathbf{\Omega}(\mathbf{\Theta}), \tag{26}$$

where $\mathbf{L}_{reg}(\mathbf{\Theta})$ is the regularized loss function, $\mathbf{L}(\mathbf{D}, \mathbf{H}, \mathbf{\Theta})$ is the loss function without regularization, $\mathbf{\Omega}(\mathbf{\Theta})$ is the penalty term, $\boldsymbol{\lambda}$ is the regularization coefficient.

Expression (26) allows you to control the complexity of the model and prevent it from overfitting by adding a model complexity penalty to the usual loss function. Regularization helps create a more robust model that generalizes better to data and is less prone to overfitting because its $\mathbf{L}(\mathbf{D}, \mathbf{H}, \mathbf{\Theta})$ component estimates the model's error on the training data set and aims to minimize the difference between predicted and actual values, $\mathbf{\Omega}(\mathbf{\Theta})$ penalizes the model for complexity and is usually expressed in terms of the norm of the model parameters (for example, L_1- or L_2-norm) or other measures of model complexity – the number of parameters, and the hyperparameter $\boldsymbol{\lambda}$ adjusts the contribution of regularization compared to the main loss function, with larger values of $\boldsymbol{\lambda}$ increasing penalizes model complexity, resulting in simpler models, while small values of $\boldsymbol{\lambda}$ allow the model to better fit the data.

To prove that the iterative process of minimizing the loss function using gradient parameter updating methods guarantees approximation to the local optimum, it is assumed that the neural network training process using the Kalman filter and regularization algorithm is based on iterative updating of the network parameters:

$$\mathbf{\Theta}_{t+1} = \mathbf{\Theta}_t - \eta \cdot \nabla \mathbf{L}_{reg}(\mathbf{\Theta}_t), \tag{27}$$

where Θ_t is the network parameters at iteration t, η is the training rate.

The iterative process of minimizing the loss function using gradient methods ensures that the local optimum of the loss function is approached, since the gradient of the loss function $\nabla L_{reg}(\Theta_t)$ indicates the direction of the fastest increase in the loss function, and the gradient at the current point Θ_t is calculated to understand how to update the model parameters to reduce the loss function. The parameter η determines the size of the step that is taken in the direction of the antigradient, which allows it to control the rate of convergence: large values of η can speed up training but can lead to divergence, and values that are too small can slow down the training. Subtracting the product of the gradient and the training rate $\nabla L_{reg}(\Theta_t)$ from the current parameters Θ_t brings the parameters closer to the local minimum of the loss function. This occurs by moving in the direction of the fastest decreasing loss function.

Thus, incorporating Chebyshev points into the Kalman filter algorithm, along with techniques such as regularization and gradient descent, aims to enhance traditional Kalman filters' performance in handling complex real-world scenarios. Chebyshev points improve the numerical stability and convergence of the filter by providing better approximations for integrals, especially in nonlinear contexts. Regularization helps prevent overfitting and ensures that the filter's parameters remain within reasonable bounds. Gradient descent optimizes the filter's performance by iteratively minimizing the error function. Together, these improvements help the Kalman filter algorithm more effectively manage nonlinearities and noise, leading to more accurate and reliable fault detection and parameter estimation in dynamic and challenging environments.

3. Experiment

For the computational experiment, we utilized a personal computer equipped with an AMD Ryzen 5 5600 processor featuring 6 cores and 12 threads, operating at 3.3 GHz, along with 32 GB of DDR-4 RAM, and running the Windows operating system. At the first stage of the computational experiment, the creation, analysis and pre-processing of a training sample is carried out, consisting of the following parameters that are recorded on board the helicopter (table 9): n_{TC} is the gas generator rotor speed, n_{FT} is the free turbine rotor speed, T_G is the gas temperature in front of the compressor turbine, h is the flight altitude, T_N is the temperature, P_N is the pressure, ρ is the air density [28, 29].

Table 9. Training sample fragment (author's research, published in [28, 29])

Number	Gas generator rotor r.p.m., n_{TC}	Free turbine rotor speed, n_{FT}	Gas temperature in front of the compressor turbine, T_G
1	0.929	0.943	0.932
2	0.933	0.982	0.964
3	0.952	0.962	0.917
4	0.988	0.987	0.908
5	0.991	0.972	0.899
6	0.997	0.963	0.915
7	0.968	0.962	0.922
8	0.962	0.969	0.989
9	0.954	0.947	0.954
…	…	…	…
256	0.973	0.981	0.953

A comprehensive account of the preprocessing steps for the training dataset is provided in [28, 29]. This preprocessing involves evaluating dataset homogeneity, splitting it into control and test samples, and assessing their representativeness through cluster analysis. Homogeneity is determined by the Fisher-Pearson test [42], which uses observed frequencies and compares them against critical values of χ^2 with degrees of freedom $r - k - 1 = 13$ and a significance level $\alpha = 0.05$. The computed χ^2 value of 3.588 is below the critical value of 22.362, affirming sample consistency and supporting the normal distribution hypothesis. Additionally, the Fisher-Snedecor test [43], which evaluates the ratio of larger to smaller variance values, yielded a criterion value of 1.28, less than the critical value of 3.44, further validating sample homogeneity. Cluster analysis was employed to assess the representativeness of both training and test samples, revealing eight distinct classes (see Fig. 4) [44–47]. After randomization, the samples were split into a 2:1 ratio (67 % training, 33 % test). Cluster analysis of both sets showed identical class distributions and similar cluster distances, underscoring their representativeness.

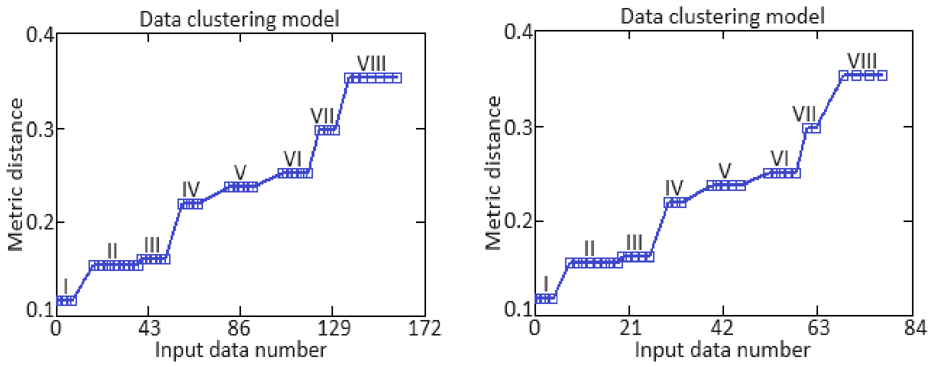

(a) (b)

Fig. 4. Diagrams of clustering results (highlighted I ... VIII classes) on initial experimental (a) and training (b) samples (author's research, published in [28, 29])

Kalman filters are typically applied to ergodic processes that operate in noisy environments, characterized by constant dispersion and zero mean [21, 25]. To validate the ergodicity of the process during preprocessing, Slutsky's condition was assessed. This condition stipulates that the autocovariance function of an ergodic process should approach zero as the lag increases. The analysis results for parameters n_{TC}, n_{FT}, T_G depicted in Fig. 5, support the hypothesis that the observed processes exhibit ergodic behavior.

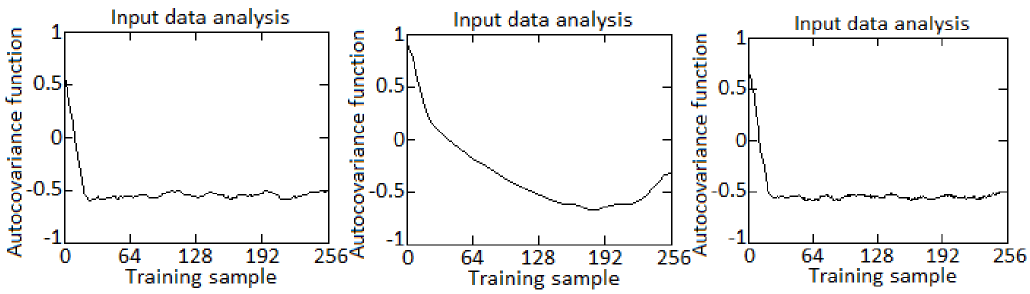

(a) (b) (c)

Fig. 5. Diagrams of autocovariance functions of parameters n_{TC} (a), n_{FT} (b), T_G (c) (author's research, published in [21])

Analysis of real noise obtained from flight testing data of the TV3-117 turboshaft engine showed that they are all characterized by zero mathematical expectation, constant dispersion and identical spectra when studying one long-duration sample and several samples. Thus, the hypothesis of ergodicity of the processes under consideration was again confirmed, since the values of the mathematical expectation and dispersion are the same both in time and in the number of implementations.

All this allows us to conclude that it is possible to use the proposed Kalman filter algorithm using Chebyshev points for this class of tasks – the task of diagnosing and countering failures of the measuring channels of automatic control systems of complex dynamic objects.

At the first stage of the computational experiment, the training curve of the modified recurrent neural network was constructed (fig. 6) to analyze changes in the loss function on the training and validation data sets depending on the number of training iterations, which helps to evaluate the effectiveness of training and identify overtraining or undertraining of the model.

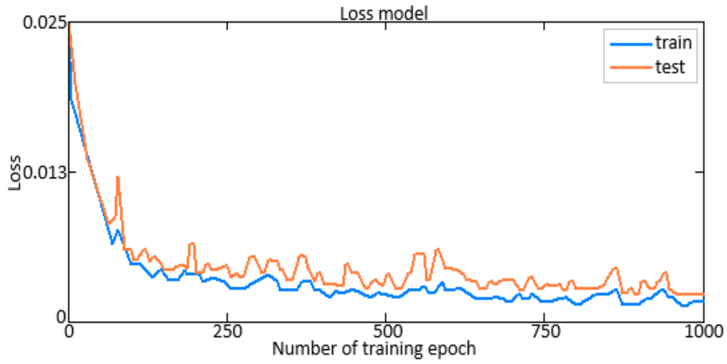

Fig. 6. Diagram of changes in the loss function of a modified recurrent neural network (author's research)

As can be seen from Fig. 6, the loss function on both the training and validation data sets remains stable over 1000 training epochs and does not go beyond the limits from –0.025 to +0.025 (from –2.5 % to +2.5 %), which indicates virtually zero risk of overfitting or undertraining of the model.

Fig. 7 shows a diagram of the distribution of the accuracy metric on the training and validation data sets depending on the number of training iterations, from which it follows that during 1000 training epochs the accuracy metric reaches the value of 1 and, as a result, the model demonstrates a high degree of training and can make accurate predictions on a given data set (table 9).

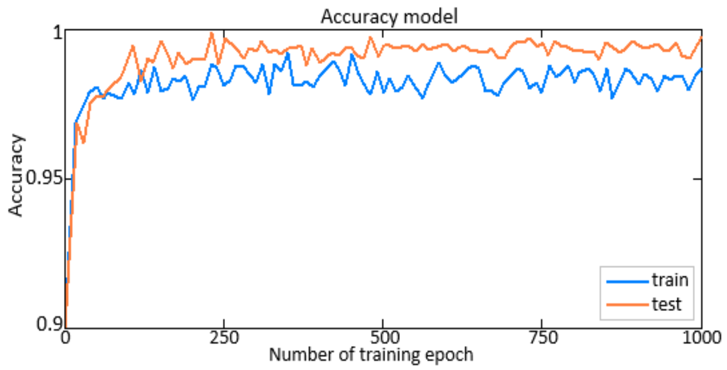

Fig. 7. Diagram of changes in the accuracy metric of a modified recurrent neural network (author's research)

Table 10 shows the average values of the model training results, as well as the value of the mathematical expectation and variance for the accuracy indicator, from which it can be seen that the main indicators of the model training results are high, which indicates the correctness of the developed algorithm for training a modified recurrent neural network.

Table 10. Average values of indicators of training results of a modified recurrent neural network (author's research)

Failure diagnostic accuracy	Failure parry accuracy	System state assessment accuracy	Average accuracy
0.99802	0.99796	0.99798	0.99799
F-measure	Precision	Recall	Dispersion accuracy
0.98572	0.96371	1.0	0.0000085

4. Results

In the Labview software environment, special software has been developed that implements a model of three channels for measuring parameters of the TV3-117 turboshaft engine with three sensors: gas-generator rotor r.p.m. sensor (D-2M), free turbine rotor speed sensor (D-1M), gas temperature sensor in front of the compressor turbine (14 dual thermocouples T-102) [48] (fig. 7).

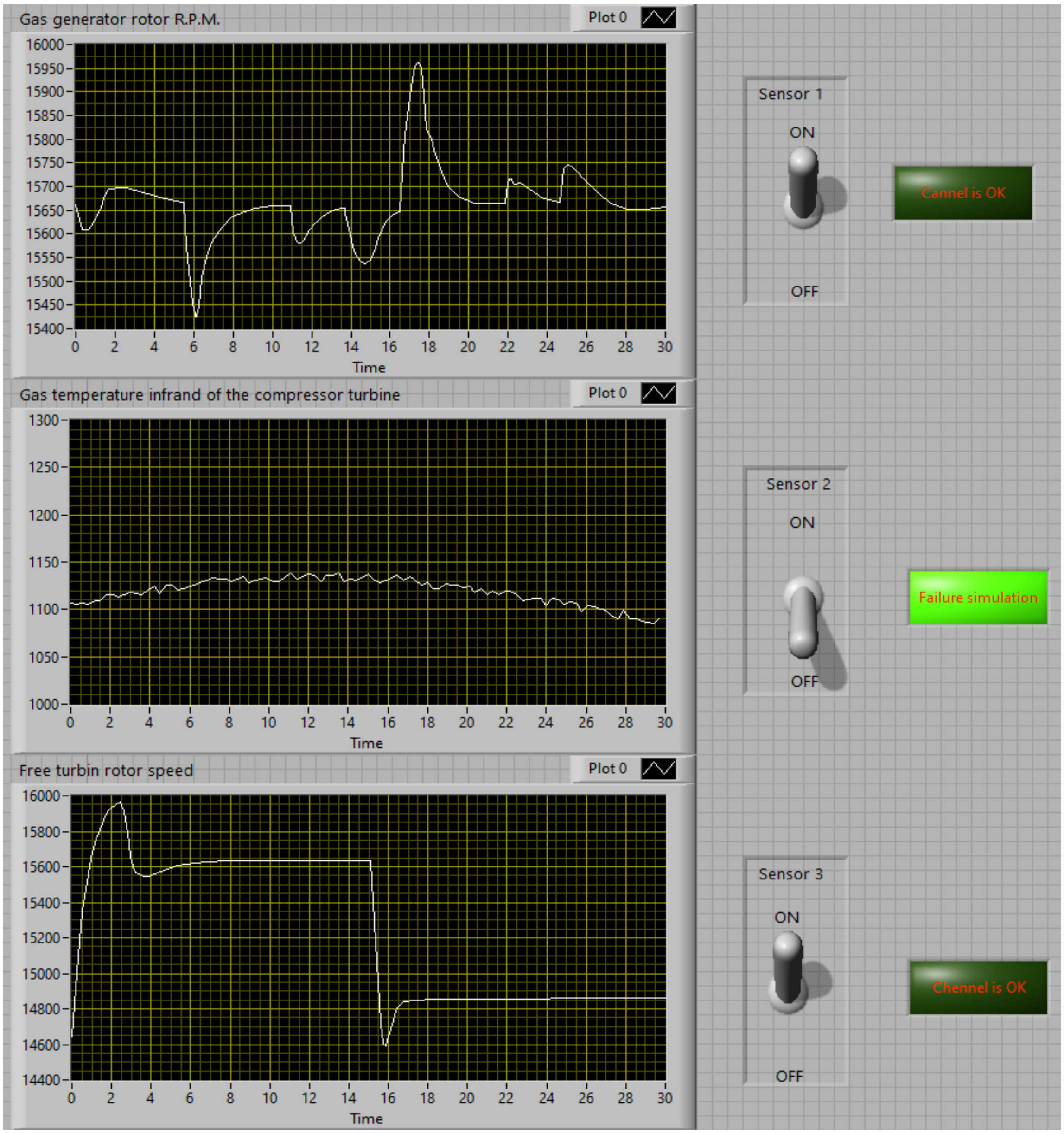

Fig. 8. Virtual installation in the LabVIEW software package, simulating a system with three sensors (author's research)

This work examines the gas temperature measuring channel in front of the compressor turbine (14 dual T-102 thermocouples). Fig. 9 shows the results of the computer simulation of the proposed Kalman filter with Chebyshev points (white curve – original signal from the sensor, that is, measured values, red curve – reconstructed signal by the neural network, that is, the model value, green curve – parameter values at the output of a multidimensional Kalman filter with Chebyshev points). The purpose of using the proposed multidimensional Kalman filter with Chebyshev points is to determine the most probable value of the real parameter measured with their help – its optimal estimate, obtained taking into account the “noisy” model (predicted) value and sensor measurements.

In line with [21, 25], the next phase of the computational experiment involved simulating the coordinate vector-column indicators for the gas temperature sensor located in front of the compressor turbine under noisy conditions. This noise included Gaussian disturbances, actual experimental flight data noise from the TV3-117 turboshaft engine, high-frequency sinusoids, and combined noise. Fig. 10 illustrates the results of filtering under combined noise for various input signals across the full operating range (acceleration, operating mode, reset) for the gas temperature in front of the compressor turbine. The white curve represents the temporal variation of the coordinate vector of the input data for model values n_{TC}, n_{FT}, T_G. The red curve shows the temporal variation for the sensor-measured values n_{TC}, n_{FT}, T_G. The green curve depicts the optimal coordinate estimates n_{TC}, n_{FT}, T_G obtained with a traditional multidimensional Kalman filter using a radial basis function neural network. Finally, the blue curve represents the optimal coordinate estimates n_{TC}, n_{FT}, T_G, obtained with a traditional multidimensional Kalman filter using a radial basis function neural network. Finally, the blue curve represents the optimal coordinate estimates n_{TC}, n_{FT}, T_G, derived from the proposed multidimensional Kalman filter with Chebyshev points and a modified recurrent neural network.

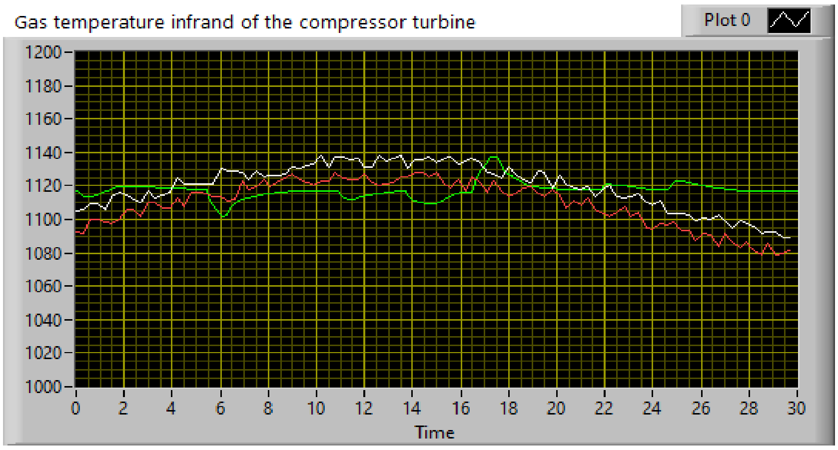

Fig. 9. Virtual installation in the LabVIEW software package, simulating a system with three sensors (author's research)

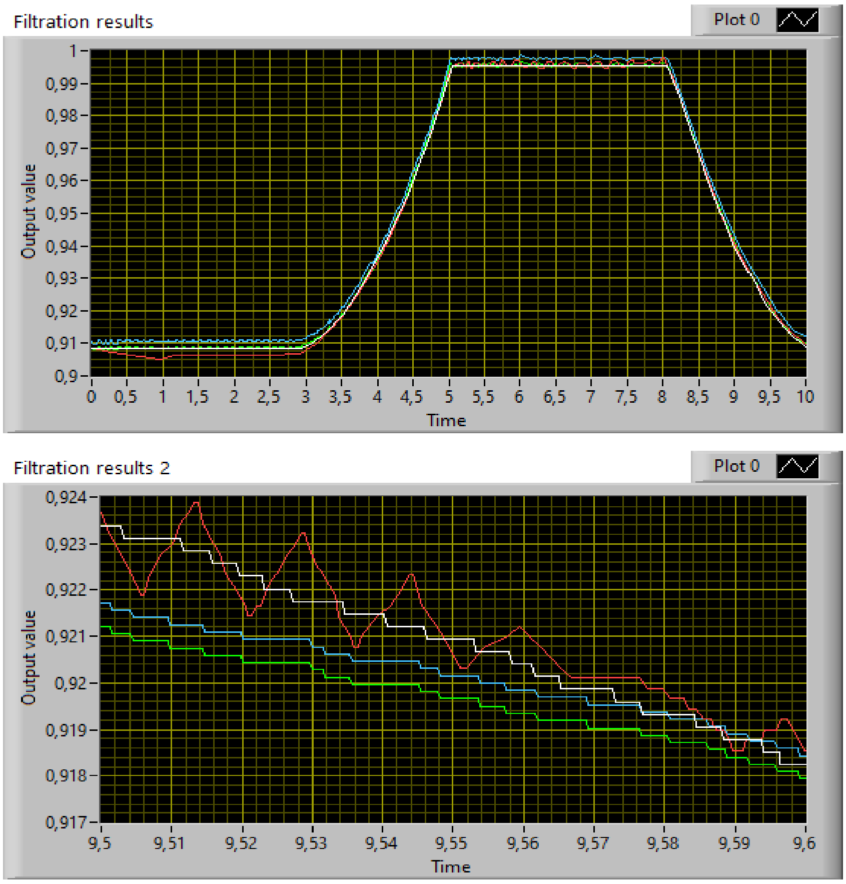

Fig. 10. Results of application of the proposed multidimensional Kalman filter with Chebyshev points in operating mode under conditions of combined noise (author's research)

The conducted studies showed that the relative error of the signals at the output of the model of the proposed multidimensional Kalman filter with Chebyshev points for coordinates n_{TC}, n_{FT}, T_G does not exceed 0.125 %, which corresponds to the established technical requirements for identification accuracy, while when using the traditional multidimensional Kalman filter it was 0.25 % in [21] and 0.5 % in [25]. The results obtained indicate a reduction in signal error by 2 times compared to [21] and 4 times compared to [26].

At the next stage of the computational experiment, according to the calculated WSSR values, similarly to [22, 23, 25, 26], situations were simulated when all measurement channels n_{TC}, n_{FT}, T_G are operational (taking into account a signal with a lower WSSR for detecting and localizing a failure) and the case of a T_G channel failure, which occurred at time t = 2.1 s (taking into account the signal from a working sensor to identify and localize a failure) (fig. 11, where white curve – model value; red and green curves – measurement of the first and second channels; blue curve – output signal). In this case, the value of the dosing needle piston is determined by the expression:

$$X_{dn} = k_1 \cdot n_{TC} \cdot k_2 \cdot n_{FT} \cdot k_3 \cdot e^{-k_4 \cdot T_G^*}, \tag{28}$$

where X_{dn} is the position signal of the metering needle piston, k_1, k_2, k_3, k_4 are coefficients that are selected empirically; for the class of helicopters TE, the following values are recommended by analyzing experimental research: k_1 = 0.001, k_2 = 1.2, k_3 = 0.8, k_4 = 0.002 [49, 50].

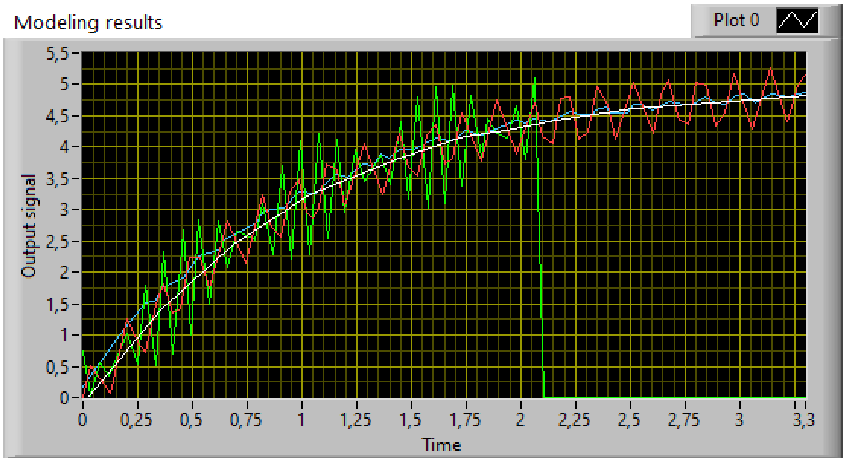

Fig. 11. Results of modelling situations when both measuring channels of a three-channel sensor are operational and when the second channel is faulty (author's research, based on [22])

According to [23, 27], one of the priority tasks of TV3-117 turboshaft engine ACS is to ensure the stability of the engine operating parameters by accurately adjusting the fuel supply (fuel consumption – G_T) to the combustion chamber to ensure the reliability of the input data of the TV3-117 turboshaft engine model. For this purpose, information flows are filtered using a reliable filtering unit containing a mathematical model of the dosing needle channel. This model allows you to obtain calculated fuel consumption values based on a certain position of the metering needle piston. The predictive (model) value of the piston position X_{dn} is the output signal of the metering needle model. According to [23, 27], the transfer function of the dosing needle is represented as:

$$W_{dn}(p) = \frac{X_{dn}^{giv}}{X_{dn}} = \frac{1}{0{,}1p+1}. \tag{29}$$

Considering that the TV3-117 turboshaft engine ACS is subject to interference both during the modelling process (caused by its inaccuracy) and during measurements (caused by sensor errors), to ensure accurate identification of the G_T control signal, it is proposed to use a multidimensional Kalman filter with Chebyshev points. Its key property is the ability to effectively correct errors in estimates of system states under conditions of uncertainty and unpredictable changes in parameters. Correction algorithms are based on determining the optimal Kalman coefficient K_k at the current moment in time by minimizing the mathematical expectation of the squared error of the parameter $\min M\left(e_{k+1}^2\right)$, taking into account the previous estimate. This coefficient forms the distribution of the model and measured components for the optimal estimate of X_{dn}. The multidimensional Kalman filtering algorithm [23, 27] includes calculations of the following statistical criteria at each stage:

$$M\left(e_{k+1}^2\right) = \frac{\sigma_{\eta_k}^2\left(M\left(e_k^2\right)+\sigma_{\xi_k}^2\right)}{M\left(e_k^2\right)+\sigma_{\xi_k}^2\cdot\sigma_{\eta_k}^2}, \tag{30}$$

$$K_{k+1} = \frac{M\left(e_k^2\right)+\sigma_{\xi_k}^2}{M\left(e_k^2\right)+\sigma_{\xi_k}^2\cdot\sigma_{\eta_k}^2}, \tag{31}$$

$$X_{dn_{k+1}}^{opt} = K_{k+1}\cdot Z_{dv_{k+1}} + \left(1-K_{k+1}\right)\cdot\left(X_{dn_k}^{opt}+\Delta X_{dn_k}\right), \tag{32}$$

where $M\left(e_{k+1}^2\right)$ is the minimum value of the mathematical expectation of the squared error; ξ_k, η_k is the model and sensor errors; K_{k+1} is the Kalman coefficient; σ_{ξ_k}, σ_{η_k} is the variances of the model and sensor; $X_{dn_k}^{opt}$ is the optimal assessment of the identified piston displacement value; z_k is the reading of the piston movement sensor; $X_{dn_k} = X\Delta t$ is the increment of piston movement obtained at the $(k + 1)$-th step using the developed mathematical model of the dosing needle.

The joint solution of equations (32)–(33) led to the derivation of the transfer function of the Kalman filter, which is equal to 1, that is, $W_K(p) = 1$.

The quality of filtration largely depends on the accuracy of measurements of the movement of the piston of the dosing needle. The use of hardware redundancy involves repeated measurement using a dual-sensor system. An important task is to ensure the reliable identification of faulty information channels. It is proposed to introduce additional fault detection and localization logic into the proposed Kalman filtering algorithm with Chebyshev points, which helps to increase reliability. From the output of the filtration unit, capable of self-correction in the event of failures (with an algorithm for detecting and localizing faults), a signal about the position of the piston is sent to a differential valve (pressure regulator), the mathematical basis of which is based on the following expressions [23, 27]:

$$G_{T_1} = G_T + \Delta G_T, \tag{33}$$

$$\frac{dG_T}{dt} = \frac{1}{T_1} \cdot \left(G_{T_1} - G_T \right), \tag{34}$$

where $T_1 = 0.05$ s, and depending on $\Delta G_T = f(X_{dn})$, $G_{T_1} = f\left(X_{dn}\right)$ are given in the form of experimental tables. The output parameter of the differential valve is the fuel consumption G_T, supplied to the input of the TV3-117 turboshaft engine model.

An important indicator of the reliability of a system is its stability, determined by the type of frequency characteristics of the systems. Therefore, to analyze the reliability of the system, the logarithmic amplitude- and phase-frequency characteristics (LAFC and LPFC) of the connection of elements, including a Kalman filter with a built-in failure detection and localization unit, and a differential valve (pressure differential regulator, which is influenced by n_{TC}, n_{FT}, T_G), are shows in fig. 12, where the X_{dn} signal from the output of the mathematical model of the dosing needle (29) is supplied to the input of the serial connection of the elements; the output is a fuel consumption signal G_T.

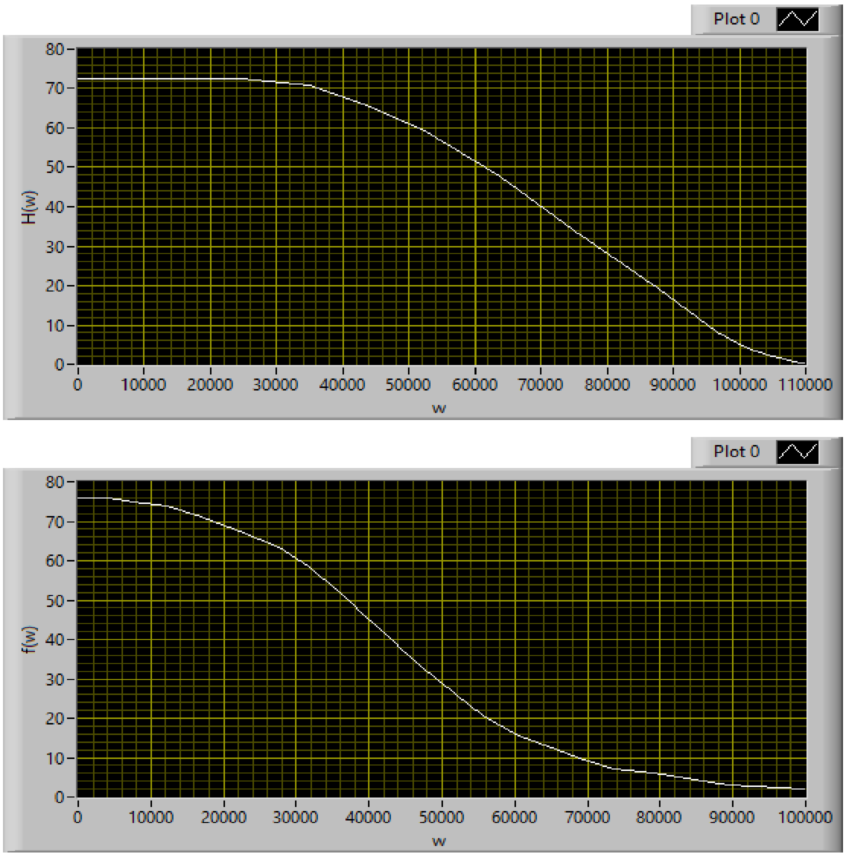

Fig. 12. LAFC and LPFC models of the failure detection and localization unit (author's research)

The LAFC and LPFC obtained as a result of the model experiment correspond to a classical first-order aperiodic link with parameters (similar to those in [23, 27]):

- the gain is determined with 20lg(k) = 46 dB and is equal to $k \approx 200$;
- time constant $T_2 = \dfrac{1}{\omega_2} = 0,05\,s$,
- the slope of the LAFC at $\omega > \omega_1$ is approximately equal to –20 dB/dec, as in [23, 27]);
- the cutoff frequency is determined by $L\left(\omega_{cf}\right) \approx 20\lg\left(\dfrac{k}{T \cdot \omega_{cf}}\right) = 0$ and is equal to $\omega_{cf} = \dfrac{k}{T} \approx 4 \cdot 10^3$ rad/s ;
- the phase over the entire frequency range varies from 0 to –90 °;
- phase value at the cutoff frequency $\theta_{cf} = -\mathrm{arctg}\left(T_1 \cdot \omega_{cf}\right) \approx -90^{\circ}$.

The transfer function of the considered connection of elements is similar to the transfer function of a differential valve (pressure regulating device), and in [23, 27] is determined according to the expression:

The transfer function of the considered connection of elements is similar to the transfer function of a differential valve (pressure regulating device), and in [23, 27] is determined according to the expression:

$$W_2\left(p\right) = \frac{G_T\left(p\right)}{X_{dn}\left(p\right)} = \frac{200}{0,05 \cdot p + 1}. \quad (35)$$

This indicates the correctness of the analytical transformations, which made it possible to obtain the transfer function of the Kalman filter equal to 1. In addition, the results of model tests allow us to conclude that $W_{FDL}(p) = 1$. Thus, the mathematical expression (35) determines the general transfer function of the fault-tolerant input block input information of the TV3-117 turboshaft engine model.

As in [23, 27] the roots of the characteristic equation of the considered block of introduction $p_1 = -10$ s^{-1}, $p_2 = -20$ s^{-1} – real and negative, then it is a second-order aperiodic link. The LAFC and LPFC characteristics of the fault-tolerant information input unit are shown in Fig. 13.

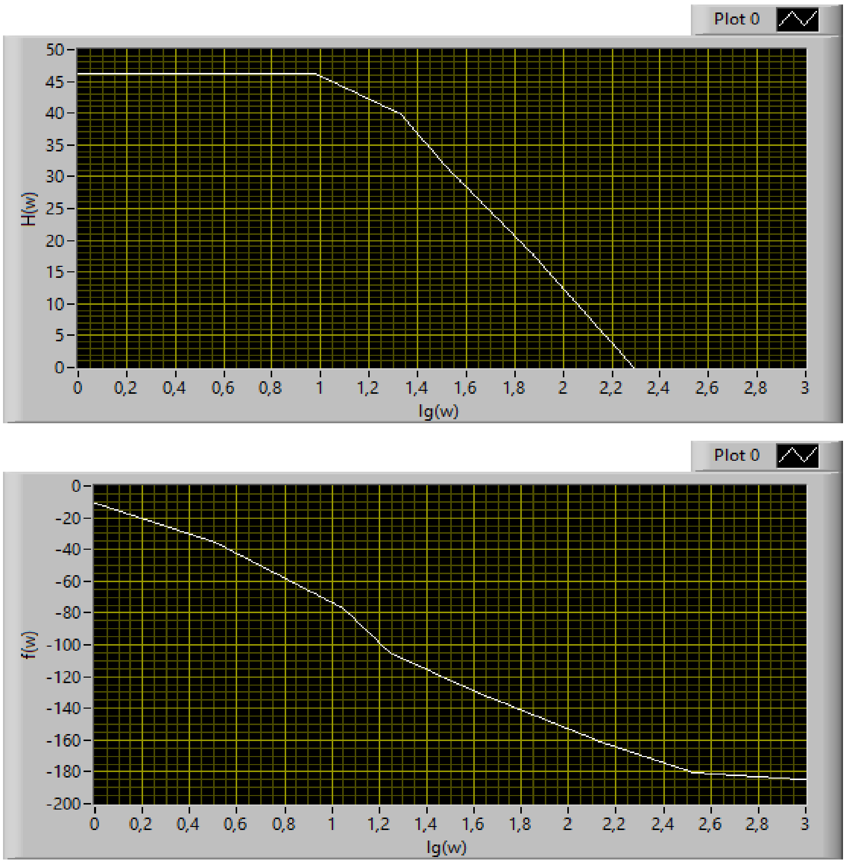

Fig. 13. LAFC and LPFC models of the failure detection and localization unit (author's research)

The block in question is covered by feedback through the ACS, which increases its stability margin, and its parameters of the fault-tolerant information input block are similar to [23, 27] and are equal to:

- the gain is determined with 20lg(k) = 46 dB and is equal to $k \approx 200$;
- time constants $T_2 = \frac{1}{\omega_2} = 0,05\ s$, $T_1 = \frac{1}{\omega_1} = 0,1\ s$;
- the slope of the LAFC for $\omega_1 < \omega < \omega_2$ is equal to –20 dB/dec, and for $\omega > \omega_2$ it is equal to –40 dB/dec.
- the cutoff frequency is determined from $L\left(\omega_{cf}\right) \approx 20 \cdot \lg\left(\frac{k}{T_1 \cdot T_2 \cdot \omega_{cf}}\right) = 0$ and is equal to $\omega_{cf} = \frac{k}{T_1 \cdot T_2} \approx 200$ rad/s;
- the phase over the entire frequency range varies from 0 to –180 °;
- phase value at the cutoff frequency $\theta_{cf} = -\mathrm{arctg}\left(\left(T_1 \cdot \omega_{cf}\right) + \mathrm{arctg}\left(T_2 \cdot \omega_{cf}\right)\right) \approx -180^{\circ}$.

Thus, an important result of the research on frequency characteristics is confirmation that the gain of the developed failure detection and localization unit is equal to unity, and there are no additional phase shifts caused by possible pure delay due to the features of the applied failure detection algorithms in the measuring channels and Kalman filtering of the input channels data from the TV3-117 turboshaft engine model. Thus, their insignificant impact on the stability of the automatic control system of the TV3-117 turboshaft engine is demonstrated.

Testing the effectiveness of the proposed multidimensional Kalman filter algorithm with Chebyshev points showed that the average relative error in dynamics is 0.124 %, and in statics at maximum fuel consumption G_T = 330 kg/h it decreases to 0.097 %. This meets modern requirements for the accuracy of identification algorithms in the fuel dosing circuit of helicopters TE, including the TV3-117 turboshaft engine.

To validate the results, a k-fold cross-validation method was employed [52–56]. The entire dataset is partitioned into k = 5 equally sized (or nearly equal) folds. Denote the dataset as D (table 9), and let D_1, D_2, …, D_k represent these individual folds. The i-th fold is used as the validation set. The remaining $k - 1$ folds are combined to form the training set. Denote the training set for i-th fold as $D_{train,i} = \bigcup_{j \neq i} D_j$. The model is trained on $D_{train,i}$ and evaluated on D_i. The performance metric M_i (mean squared error) is calculated for the model's predictions on the i-th fold's validation set. The overall performance metric $\overline{M}$ is computed by averaging the metrics obtained from each fold [57, 58]:

$$\overline{M} = \frac{1}{k} \cdot \sum_{i=1}^{k} M_i, \tag{36}$$

where $\overline{M}$ represents the mean performance metric across all folds.

The training dataset was partitioned randomly into five equal segments (folds), each comprising 51 data points. The computed metric values for these segments were: M_1 = 0.0024, M_2 = 0.0023, M_3 = 0.0026, M_4 = 0.0024, and M_5 = 0.0024. The mean metric $\overline{M}$ across all folds was determined to be 0.00242, which is 3.2 % greater than the minimum MSE_{min} = 0.0025 recorded from the first fold (k_1). This suggests that the average MSE derived from cross-validation closely approximates the optimal MSE observed in a single fold. The 3.2 % deviation indicates the extent to which the average metric diverges from the best individual result obtained during the cross-validation. Furthermore, these results illustrate the model's robustness, as the difference between the average metric and MSE_{min} is relatively small. It is essential to note that while the average metric offers a general view of the model’s performance across the entire training set, MSE_{min} represents the most favourable outcome achieved within a particular subset of the data.

The results have practical significance for evaluating and improving predictive models. The close match between the average metric and the minimum MSE demonstrates the model's reliability and consistency, crucial for applications like fault detection systems. This consistency ensures the model's predictions are stable across various conditions. Understanding the difference between the average metric and the best MSE aids in model optimization, helping to refine performance and enhance the effectiveness of systems that depend on these models.

5. Discussion

At the first stage of the comparative analysis of the proposed method for diagnosing and fending off failures in the measurement channels of automatic control systems of complex dynamic objects (using the example of the TV3-117 turboshaft engine) with known ones, errors of the 1st and 2nd types were assessed (table 11) for the proposed multidimensional filter algorithm Kalman with Chebyshev points without using neural networks, as in [25], using a neural network of radial basis functions, as in [21], and using the proposed modified recurrent neural network. A comparative analysis showed that the use of a modified recurrent neural network reduces errors of the 1st and 2nd types by 1.24...1.71 times in comparison with the use of a neural network of radial basis functions [21] and by 1.70...2.90 times in comparison without the use of neural networks [25].

Table 11. Results of calculating errors of the 1st and 2nd types (author's research)

Identification method based on the multivariate Kalman filter	The probability of an error in the identification of parameters					
	n_{TC}		n_{FT}		T_G	
	The error of the first kind	The error of the second kind	The error of the first kind	The error of the second kind	The error of the first kind	The error of the second kind
Without using neural networks [25]	0.84	0.63	0.85	0.64	0.79	0.58
Using the RBF network [21]	0.62	0.38	0.63	0.41	0.56	0.33
Using a modified recurrent neural network	0.49	0.23	0.50	0.24	0.45	0.20

At the next stage of the comparative analysis of the proposed method for diagnosing and parring off failures in the measurement channels of automatic control systems of complex dynamic objects (using the example of the TV3-117 turboshaft engine) with the known ones, the calculation of the main metrics for the proposed method was carried out using a modified recurrent neural network, a neural network of radial basis functions [21] and a multidimensional Kalman filter without a neural network implementation [25] (table 12).

Table 12. Results of comparative analysis (author's research)

Metrics	The proposed method using a modified recurrent neural network	The method developed in [21] uses a neural network of radial basis functions.	The method developed in [25] without a neural network implementation.
Standard deviation $MSE = \frac{1}{N} \cdot \sum_{i=1}^{N} \left(y_i - y_i \right)^2$	0.00226	0.00372	0.00498
Mean absolute error $MAE = \frac{1}{N} \cdot \sum_{i=1}^{N} \left\| y_i - y_i \right\|$	0.03081	0.03526	0.03884
Mean absolute percentage error $MAPE = \frac{1}{N} \cdot \sum_{i=1}^{N} \left\| \frac{y_i - y_i}{y_i} \right\| \cdot 100\%$	1.158 %	1.833 %	2.036 %
Coefficient of determination R^2, which evaluates the model’s ability to accurately reproduce previous data	0.976	0.919	0.883
Coefficient of determination R^2, which evaluates the model’s ability to accurately predict future values	0.975	0.872	0.841
Adaptability	The advantage of the modified recurrent neural network over the radial basis function neural network and the multidimensional Kalman filter is its ability to take into account long-term dependencies in the data due to internal memory and feedback. This allows the modified recurrent neural network to more efficiently model sequential data such as time series or text and make accurate predictions, especially in the face of variables or complex internal data structures.		
Robustness	The advantage of a modified recurrent neural network over a radial basis function neural network and a multidimensional Kalman filter is its ability to take into account sequential dependencies in temporal data and adapt to changes in data dynamics. Thanks to internal memory and feedback, a modified recurrent neural network can process information about past states and use this information to make predictions about future values. This allows the modified recurrent neural network to respond more flexibly to noise and unexpected changes in data, making it more robust and reliable in a variety of conditions, including situations with incomplete or noisy data.		

As can be seen from table 12, the results of a comparative analysis confirm the effectiveness of using a modified recurrent neural network in the method of diagnosing and fending off failures of the measuring channels of complex dynamic objects ACS in front of a neural network of radial basis functions [21] and a multidimensional Kalman filter without a neural network implementation [25], as evidenced by the minimum value of the standard deviation, mean absolute error, mean absolute percentage error, as well as the maximum value of the coefficient of determination to assess the accuracy of the model’s ability to both reproduce previous data and predict future values. In addition, significant advantages of the modified recurrent neural network over the neural network of radial basis functions [21] and the multidimensional Kalman filter without a neural network implementation [25] in the context of its adaptability and robustness are highlighted [59].

To implement the advanced Kalman filter with Chebyshev points onboard a helicopter, a comprehensive integration of sensors and real-time processing software is required. The system should incorporate rotor speed sensors, gas temperature sensors, and other relevant instrumentation to monitor engine parameters continuously. The LabVIEW-based software, featuring the proposed multidimensional Kalman filter, will be embedded in the helicopter's onboard diagnostic system. This filter, enhanced by Chebyshev points, will refine sensor data and provide precise estimates of engine parameters by addressing nonlinearity and noise. The neural network component will further improve the filter's performance, enabling real-time data correction and fault detection.

The onboard diagnostic system will utilize the filtered data to identify and mitigate sensor faults effectively. The system will monitor deviations from expected parameter ranges and activate predefined responses, such as recalibration or switching to backup sensors, to ensure operational reliability. Regular validation and calibration against flight data will maintain the accuracy and adaptability of the filter and neural network, thereby enhancing overall system safety and efficiency. This integration of advanced filtering techniques and neural network capabilities aims to significantly improve sensor data accuracy, fault detection, and mitigation processes in dynamic and challenging flight conditions.

6. Conclusions

1. The method for diagnosing and parring off failures of the measuring channels of complex dynamic objects automatic control system was further developed, which differs from existing ones in that, through the use of a multidimensional Kalman filter with Chebyshev points, implemented by a modified recurrent neural network, it made it possible to detect and localize failures of sensors with an average accuracy 0.99799 (99.8 %).

2. For the first time, an implementation of a multidimensional Kalman filter with Chebyshev points by a modified recurrent neural network has been proposed, including an input layer, a failure diagnostics layer, a failure parry layer, a filtering and smoothing layer, a results aggregation layer, the use of which is used to solve the main problems of the method of diagnosing and parrying failures of the system's measuring channels complex dynamic objects automatic control system, such as diagnostics of failures with an accuracy of 0.99802, fending off failures with an accuracy of 0.99796, assessment of the state of a system with an accuracy of 0.99798.

3. It has been experimentally proven that the use of a modified recurrent neural network, including an input layer, a failure diagnostics layer, a failure parry layer, a filtering and smoothing layer, a result aggregation layer, to implement a multidimensional Kalman filter with Chebyshev points reduces the errors of the 1st and 2nd kind 1.24...1.71 times in comparison with the use of a neural network of radial-basis functions and 1.70...2.90 times – in comparison without the use of neural networks, in solving the problem of diagnosing and fending off failures of the measuring channels of the automatic control system of complex dynamic objects (using the example of TV3-117 turboshaft engine).

4. It is proposed to use the loss function of a modified recurrent neural network, including an input layer, a failure diagnostic layer, a failure parry layer, a filtering and smoothing layer, and a results aggregation layer, as a total loss function for fault diagnosis, for failure parry and for assessing the state of the system, which made it possible to avoid its overtraining in the presence of a large number of parameters or undertraining or a small amount of data. It has been experimentally confirmed that the loss function on both the training and validation data sets remains stable over 1000 training epochs and does not go beyond the limits from –0.025 to +0.025 (from –2.5 % to +2.5 %), which indicates virtually zero the risk of overtraining or undertraining the model.

5. By researching the frequency characteristics, the effectiveness of using a multidimensional Kalman filter with Chebyshev points, implemented by a modified recurrent neural network, including an input layer, a fault diagnostics layer, a fault parry layer, a filtering and smoothing layer, a result aggregation layer, in the problem of diagnosing and parrying failures has been experimentally confirmed measuring channels of complex dynamic objects automatic control system (using the example of the TV3-117 turboshaft engine), since the gain of the developed failure detection and localization unit is equal to unity, and there are no additional phase shifts caused by possible pure delay due to the features of the applied failure detection algorithms in the measuring channels and Kalman filtering of model input data.

6. The feasibility of using a modified recurrent neural network in the method of diagnosing and fending off failures of the measuring channels of complex dynamic objects automatic control system in front of a neural network of Radial basis functions [21] and a multidimensional Kalman filter without a neural network implementation [25], according to the metrics of standard deviation, have been an experimentally substantiated average absolute error, average absolute percentage error, coefficient of determination, which evaluates the ability of the model to accurately reproduce previous data, coefficient of determination, which evaluates the ability of the model to accurately predict future values, namely:

- the value of the standard deviation of the modified recurrent neural network is 0.00226, which is 1.65 times less than the radial basis function neural network [21] and 2.20 times less than the multidimensional Kalman filter without a neural network implementation [25];
- the value of the average absolute error of the modified recurrent neural network is 0.03081, which is 1.14 times less than the radial basis function neural network [21] and 1.26 times less than the multidimensional Kalman filter without a neural network implementation [25];
- the value of the average absolute percentage error of the modified recurrent neural network is 1.158%, which is 1.58 times less than the neural network of radial basis functions [21] and 1.76 times less than the multidimensional Kalman filter without a neural network implementation [25];
- the value of the coefficient of determination, which evaluates the ability of the model to accurately reproduce previous data, of the modified recurrent neural network is 0.976, which is 1.06 times more than the neural network of radial basis functions [21] and 1.11 times more than a multidimensional Kalman filter without a neural network implementation [25];

• the value of the coefficient of determination, which evaluates the ability of the model to accurately predict future values, of the modified recurrent neural network is 0.975, which is 1.12 times more than the neural network of radial basis functions [21] and 1.16 times more than the multidimensional Kalman filter without a neural network implementation [25].

7. A modified recurrent neural network is superior to radial basis function neural network and multivariate Kalman
8. filter due to its ability to account for long-term dependencies in data through internal memory and feedback loops, which enables more efficient modelling of sequential data such as time series and makes predictions more efficient accurate, especially in the presence of variables or complex internal data structures.
9. The modified recurrent neural network is superior to the radial basis function neural network and multivariate Kalman filter due to its ability to take into account sequential dependencies in temporal data and adapt to changes in data dynamics. Thanks to internal memory and feedback, a modified recurrent neural network can process information about past states and use this information to make predictions about future values. This allows the modified recurrent neural network to respond more flexibly to noise and unexpected changes in data, making it more robust and reliable in a variety of conditions, including situations with incomplete or noisy data. It has been experimentally proven that the relative error of the signals at the output of the modified recurrent neural network in the proposed multidimensional Kalman filter with Chebyshev points for TV3-117 turboshaft engine thermogas-dynamic parameters does not exceed 0.125 %, which corresponds to the established technical requirements for identification accuracy; at that time it was 0.50 % when using the traditional multidimensional Kalman filter [21] and 0.25 % – a neural network of radial basis functions [25].
10. The developed method, incorporating a multidimensional Kalman filter with Chebyshev points and a modified recurrent neural network, significantly enhances the precision and reliability of sensor failure diagnostics and fault mitigation in complex dynamic systems. The high accuracy achieved – 99.8% in failure detection and 99.8% in fault mitigation—demonstrates its effectiveness in real-world applications such as aerospace engine monitoring. The system's robustness against noise and its capability to provide precise diagnostics make it suitable for critical applications where reliable performance is essential, such as the real-time monitoring and maintenance of helicopter engines like the TV3-117.
11. Despite the advancements, the proposed method has certain limitations. The reliance on a modified recurrent neural network, while offering improved performance, may still be constrained by the quality and quantity of training data. Additionally, the method's performance is highly dependent on the correct configuration and tuning of the neural network and Kalman filter parameters. Variations in operational conditions or unanticipated sensor faults could affect the system’s accuracy, highlighting the need for further refinement and adaptation.
12. Future research should focus on expanding the applicability of the proposed method to a broader range of dynamic systems beyond the TV3-117 engine. Investigating the integration of advanced neural network architectures and adaptive filtering techniques could enhance the model's robustness and flexibility. Additionally, exploring the impact of varying environmental conditions and sensor characteristics on system performance will be crucial for optimizing the method's reliability and effectiveness in diverse operational scenarios.

References

[1] C. Campestrini, T. Heil, S. Kosch, A. Jossen, “A comparative study and review of different Kalman filters by applying an enhanced validation method”, *Journal of Energy Storage*, vol. 8, pp. 142–159, 2016. https://doi.org/10.1016/j.est.2016.10.004

[2] J. Siswantoro, A. S. Prabuwono, A. Abdullah, B. Idrus, “A linear model based on Kalman filter for improving neural network classification performance”, *Expert Systems with Applications*, vol. 49, pp. 112–122, 2016. https://doi.org/10.1016/j.eswa.2015.12.012

[3] Y. Li, B. Wahlberg, X. Hu, L. Xie, “Inverse Kalman filtering problems for discrete-time systems”, *Automatica*, vol. 163, 111560, 2024. https://doi.org/10.1016/j.automatica.2024.111560

[4] Q. Luo, S. Li, X. Yan, C. Wang, Z. Zhou, G. Jia, “An improved two-phase robust distributed Kalman filter”, *Signal Processing*, vol. 220, 109438, 2024. https://doi.org/10.1016/j.sigpro.2024.109438

[5] Y. Li, B. Wahlberg, X. Hu, L. Xie, “Inverse Kalman filtering problems for discrete-time systems”, *Automatica*, vol. 163, 111560, 2024. https://doi.org/10.1016/j.automatica.2024.111560

[6] X. Song, W. X. Zheng, “A Kalman-filtering derivation of input and state estimation for linear discrete-time systems with direct feedthrough”, *Automatica*, vol. 161, 111453, 2024. https://doi.org/10.1016/j.automatica.2023.111453

[7] R. Liu, M. Liu, G. Duan, X. Cao, “Robust adaptive smooth variable structure Kalman filter for spacecraft attitude estimation”, *Aerospace Science and Technology*, vol. 144, 108784, 2024. https://doi.org/10.1016/j.ast.2023.108784

[8] X. Li, A. Lei, L. Zhu, M. Ban, “Improving Kalman filter for cyber physical systems subject to replay attacks: An attack-detection-based compensation strategy”, *Applied Mathematics and Computation*, vol. 466, 128444, 2024. https://doi.org/10.1016/j.amc.2023.128444

[9] D. C. dos Santos Gomes, G. L. de Oliveira Serra, “Interval type-2 evolving fuzzy Kalman filter for processing of unobservable spectral components from uncertain experimental data”, *Journal of the Franklin Institute*, vol. 361, issue 2, pp. 637–669, 2024. https://doi.org/10.1016/j.jfranklin.2023.12.017

[10] M. Ma, L. Fu, Z. Zhai, R.-B. Sun, “Transformer based Kalman Filter with EM algorithm for time series prediction and anomaly detection of complex systems”, *Measurement*, vol. 229, 114378, 2024. https://doi.org/10.1016/j.measurement.2024.114378

[11] F. Farahi, H. S. Yazdi, “Probabilistic Kalman filter for moving object tracking”, *Signal Processing: Image Communication*, vol. 82, 115751, 2020. https://doi.org/10.1016/j.image.2019.115751

[12] A. Rahdan, H. Bolandi, M. Abedi, "Design of on-board calibration methods for a digital sun sensor based on Levenberg–Marquardt algorithm and Kalman filters", *Chinese Journal of Aeronautics*, vol. 33, issue 1, 339–351, 2020. https://doi.org/10.1016/j.cja.2019.08.011
[13] A. G. Wills, T. B. Schon, "Stochastic quasi-Newton with line-search regularisation", *Automatica*, vol. 127, 109503, 2021. https://doi.org/10.1016/j.automatica.2021.109503
[14] M. Ihme, W. T. Chung, A. A. Mishra, "Combustion machine learning: Principles, progress and prospects", *Progress in Energy and Combustion Science*, vol. 91, 101010, 2022. https://doi.org/10.1016/j.pecs.2022.101010
[15] H. Yousefnejad, M. S. Monfared, "A control algorithm for a non-stationary batch service production system using Kalman filter", *Expert Systems with Applications*, vol. 207, 117916, 2022. https://doi.org/10.1016/j.eswa.2022.117916
[16] C. A. Gomez-Uribe, B. Karrer, "The Decoupled Extended Kalman Filter for Dynamic Exponential-Family Factorization Models", *Journal of Machine Learning Research*, vol. 22, pp. 1–15, 2022. URL: https://www.jmlr.org/papers/volume22/18-417/18-417.pdf
[17] T. M. Chin, "Square-Root Formulas for Kalman Filter, Information Filter, and RTS Smoother: Links via Boomerang Prediction Residual", *IPN Progress Report*, vol. 42-233, pp. 1–23, 2023. URL: https://ipnpr.jpl.nasa.gov/progress_report/42-233/42-233A.pdf
[18] Q. Ge, Y. Cheng, G. Yao, S. Chen, Y. Zhu, "Credible Gaussian sum cubature Kalman filter based on non-Gaussian characteristic analysis", *Neurocomputing*, vol. 565, 126922, 2024. https://doi.org/10.1016/j.neucom.2023.126922
[19] S. Zhong, B. Peng, J. He, Z. Feng, M. Li, G. Wang, "Kalman filtering based on dynamic perception of measurement noise", *Mechanical Systems and Signal Processing*, vol. 213, 111343, 2024. https://doi.org/10.1016/j.ymssp.2024.111343
[20] S. Vladov, Y. Shmelov, R. Yakovliev, M. Petchenko, "Helicopters Turboshaft Engines Parameters Identification Using Neural Network Technologies Based on the Kalman Filter", *Communications in Computer and Information Science*, vol. 1980, pp. 82–97, 2023. https://doi.org/10.1007/978-3-031-48325-7_7
[21] S. Vladov, Y. Shmelov, R. Yakovliev, M. Petchenko, Drozdova, "Neural Network Method for Helicopters Turboshaft Engines Working Process Parameters Identification at Flight Modes", in: Proceedings of the 2022 IEEE 4th International Conference on Modern Electrical and Energy System (MEES), Kremenchuk, Ukraine, October 20–22, 2022, pp. 604–609. https://doi.org/10.1109/MEES58014.2022.10005670
[22] S. Vladov, Y. Shmelov, R. Yakovliev, "Helicopters Aircraft Engines Self-Organizing Neural Network Automatic Control System", *CEUR Workshop Proceedings*, vol. 3137, pp. 28–47, 2022. https://doi.org/10.32782/cmis/3137-3 URL: https://ceur-ws.org/Vol-3137/paper3.pdf
[23] S. Vladov, R. Yakovliev, O. Hubachov, J. Rud, "Neuro-Fuzzy System for Detection Fuel Consumption of Helicopters Turboshaft Engines", *CEUR Workshop Proceedings*, vol. 3628, pp. 55–72, 2024. URL: https://ceur-ws.org/Vol-3628/paper5.pdf
[24] T. Kuznetsova, Y. Likhacheva, E. Gubarev, A. Yakushev, "The identification of gas turbine engine parameters by the multidimensional Kalman filter", *Vestnik PSTU*, no. 10, pp. 114–126, 2014.
[25] T. Kuznetsova, E. Gubarev, V. Avgustinovich, "The algorithms of measuring channels' fault diagnostics and counteraction for automatic control system of aero-engines", *Vestnik PSTU*, no. 16, pp. 5–14, 2015.
[26] T. Kuznetsova, E. Gubarev, "Fault-tolerant algorithms for identifying input information of an on-board mathematical model as part of an automatic control system for an aircraft engine", *Fundamental research*, no. 6-1, pp. 39–43, 2015.
[27] S. Vladov, R. Yakovliev, O. Hubachov, J. Rud, Y. Stushchanskyi, "Neural Network Modeling of Helicopters Turboshaft Engines at Flight Modes Using an Approach Based on "Black Box" Models", *CEUR Workshop Proceedings*, vol. 3624, pp. 116–135, 2024. URL: https://ceur-ws.org/Vol-3624/Paper_11.pdf
[28] S. Vladov, Y. Shmelov, R. Yakovliev, and M. Petchenko, "Neural Network Method for Parametric Adaptation Helicopters Turboshaft Engines On-Board Automatic Control," *CEUR Workshop Proceedings*, vol. 3403, pp. 179–195, 2023. URL: https://ceur-ws.org/Vol-3403/paper15.pdf
[29] H. Sheng, Q. Chen, J. Li, W. Jiang, Z. Wang, Z. Liu, T. Zhang, Y. Liu, "Research on dynamic modeling and performance analysis of helicopter turboshaft engine's start-up process", *Aerospace Science and Technology*, vol. 106, 106097, 2020. https://doi.org/10.1016/j.ast.2020.106097
[30] P. Yun, P. Wu, S. He, X. Li, "A variational Bayesian based robust cubature Kalman filter under dynamic model mismatch and outliers interference", *Measurement*, vol. 191, 110063, 2022. https://doi.org/10.1016/j.measurement.2021.110063
[31] J. He, G. Wang, H. Yu, J. M. Liu, B. Peng, "Generalized minimum error entropy Kalman filter for non-Gaussian noise", *ISA Transactions*, vol. 136, pp. 663–675, 2023. https://doi.org/10.1016/j.isatra.2022.10.040
[32] A. Abdulnagimov, G. Ageev, "Neural network technologies in hardware-in-the-loop simulation: principles of gas turbine digital twin development", *Informatics, Computer Science and Management*, vol. 23, no. 4 (86), pp. 115–121, 2019.
[33] Z. Liu, S. Chen, H. Wu, F. Liang, "Orthogonal Simplex Chebyshev-Laguerre Cubature Kalman Filter Applied in Nonlinear Estimation Systems", *Applied Sciences*, vol. 8 (6), 863, 2018. https://doi.org/10.3390/app8060863
[34] S. K. Biswas, L. Qiao, A. G. Dempster, "A quantified approach of predicting suitability of using the Unscented Kalman Filter in a non-linear application", *Automatica*, vol. 241, 109241, 2020. https://doi.org/10.1016/j.automatica.2020.109241
[35] K. Hoppe, F. Giesa, G. Schaldach, M. Thommes, D. Pieloth, "Optimization of filter structures by evolutionary strategies", *Materials Today Communications*, vol. 38, 108510, 2024. https://doi.org/10.1016/j.mtcomm.2024.108510
[36] O. Adigun, B. Kosko, "Noise-boosted recurrent backpropagation", *Neurocomputing*, vol. 559, 126438, 2023. https://doi.org/10.1016/j.neucom.2023.126438
[37] C. Ruiz, C. M. Alaíz, J. R. Dorronsoro, "Convex formulation for multi-task L1-, L2-, and LS-SVMs", *Neurocomputing*, vol. 456, pp. 599–608, 2021. https://doi.org/10.1016/j.neucom.2021.01.137
[38] Z. Hou, L. Yu, Y. Liang, B. Xu, Y. Lei, "Integrating L1 and weighted L2 regularization for moving force identification from combined response measurements", *Measurement*, vol. 228, 114337, 2024. https://doi.org/10.1016/j.measurement.2024.114337
[39] X. Cao, H. Luo, J. Tai, R. Jiang, G. Wang, "Multi-agent target search strategy optimization: Hierarchical reinforcement learning with multi-criteria negative feedback", *Applied Soft Computing*, vol. 149, part A, 110999, 2023. https://doi.org/10.1016/j.asoc.2023.110999

[40] E. Birihanu, “Analysis of Software Quality Using Software Metrics”, *International Journal on Computational Science & Applications*, vol. 8 (4/5), pp. 11–28, 2018. https://doi.org/10.5121/ijcsa.2018.8502

[41] F. S. Corotto, “Appendix C - The method attributed to Neyman and Pearson”, *Wise Use of Null Hypothesis Tests*, pp. 179–188, 2023. https://doi.org/10.1016/B978-0-323-95284-2.00012-4

[42] F. V. Motsnyi, “Analysis of Nonparametric and Parametric Criteria for Statistical Hypotheses Testing. Chapter 1. Agreement Criteria of Pearson and Kolmogorov”, *Statistics of Ukraine*, no. 4’2018 (83), pp. 14–24, 2018. https://doi.org/10.31767/su.4(83)2018.04.02

[43] Y.-M. Tamm, R. Damdinov, A. Vasilev, “Quality Metrics in Recommender Systems: Do We Calculate Metrics Consistently?”, in Proceedings of the 15th ACM Conference on Recommender Systems, Amsterdam, Netherlands, 27 September 2021 – 01 October 2021, pp. 708–713. https://doi.org/10.1145/3460231.3478848

[44] S. Vladov, R. Yakovliev, M. Bulakh, and V. Vysotska, “Neural Network Approximation of Helicopter Turboshaft Engine Parameters for Improved Efficiency”, *Energies*, vol. 17, issue 9, 2233, 2024. https://doi.org/10.3390/en17092233

[45] Z. Hu, O. Shkurat, and M. Kasner, “Grayscale Image Colorization Method Based on U-Net Network”, *International Journal of Image, Graphics and Signal Processing (IJIGSP)*, vol. 16, no. 2, pp. 70–82, 2024. https://doi.org/10.5815/ijigsp.2024.02.06

[46] S. Babichev, J. Krejci, J. Bicanek, and V. Lytvynenko, “Gene expression sequences clustering based on the internal and external clustering quality criteria”, in: Proceedings of the 2017 12th International Scientific and Technical Conference on Computer Sciences and Information Technologies (CSIT), Lviv, Ukraine, September 05–08, 2017. https://doi.org/10.1109/STC-CSIT.2017.8098744

[47] S. Vladov, L. Scislo, V. Sokurenko, O. Muzychuk, V. Vysotska, S. Osadchy, A. Sachenko, “Neural Network Signal Integration from Thermogas-Dynamic Parameter Sensors for Helicopters Turboshaft Engines at Flight Operation Conditions”, *Sensors*. vol. 24, issue 13, 4246, 2024. https://doi.org/10.3390/s24134246

[48] S. Vladov, R. Yakovliev, V. Vysotska, M. Nazarkevych, V. Lytvyn, “The Method of Restoring Lost Information from Sensors Based on Auto-Associative Neural Networks,” Applied System Innovation, vol. 7, no. 3. 53, 2024. https://doi.org/10.3390/asi7030053

[49] X. Liu, Y. Chen, L. Xiong, J. Wang, C. Luo, L. Zhang, K. Wang, “Intelligent fault diagnosis methods toward gas turbine: A review”, *Chinese Journal of Aeronautics*, vol. 37, issue 4, pp. 93–120, 2024. https://doi.org/10.1016/j.cja.2023.09.024

[50] S.S. Talebi, A. Madadi, A.M. Tousi, M. Kiaee, “Micro Gas Turbine fault detection and isolation with a combination of Artificial Neural Network and off-design performance analysis”, Engineering Applications of Artificial Intelligence, vol. 113, 104900, 2022. https://doi.org/10.1016/j.engappai.2022.104900

[51] S. Pang, Q. Li, B. Ni, “Improved nonlinear MPC for aircraft gas turbine engine based on semi-alternative optimization strategy”, *Aerospace Science and Technology*, vol. 118, 106983, 2021. https://doi.org/10.1016/j.ast.2021.106983

[52] A. R. Marakhimov, K. K. Khudaybergenov, “Approach to the synthesis of neural network structure during classification,” *International Journal of Computing*, vol. 19, issue 1, pp. 20–26, 2020. https://doi.org/10.47839/ijc.19.1.1689

[53] E. M. Cherrat, R. Alaoui, H. Bouzahir, “Score fusion of finger vein and face for human recognition based on convolutional neural network model,” *International Journal of Computing*, vol. 19, issue 1, pp. 11–19, 2020. https://doi.org/10.47839/ijc.19.1.1688

[54] T. E. Romanova, P. I. Stetsyuk, A. M. Chugay, S. B. Shekhovtsov, “Parallel Computing Technologies for Solving Optimization Problems of Geometric Design,” *Cybernetics and Systems Analysis*, vol. 55, no. 6, pp. 894–904, 2019. https://doi.org/10.1007/s10559-019-00199-4.

[55] Z. Hu, I. Dychka, K. Potapova, V. Meliukh, “Augmenting Sentiment Analysis Prediction in Binary Text Classification through Advanced Natural Language Processing Models and Classifiers”, *International Journal of Information Technology and Computer Science*, vol. 16, no. 2, pp. 16–31

[56] R. Peleshchak, V. Lytvyn, I. Peleshchak, D. Dudyk, D. Uhryn, “Data Clustering by Chaotic Oscillatory Neural Networks with Dipole Synaptic Connections”, *International Journal of Modern Education and Computer Science*, vol. 16, no. 3, pp. 27–38, 2024.

[57] V. Sahana, R. Shashidhar, R. Bindushree, A.N. Chandana, “IOT Based Burglar Detection and Alarming System Using Raspberry Pi”, *International Journal of Engineering and Manufacturing*, vol. 13, no. 6, pp. 23–37, 2023.

[58] S. Vladov, Y. Shmelov, R. Yakovliev, Y. Stushchanskyi, Y. Havryliuk, “Neural Network Method for Controlling the Helicopters Turboshaft Engines Free Turbine Speed at Flight Modes”, *CEUR Workshop Proceedings*, vol. 3626, pp. 89–108, 2023.

[59] S. Gudla, and K.N. Rao, “Reliable Data Delivery Using Fuzzy Reinforcement Learning in Wireless Sensor Networks”, *International Journal of Computer Network and Information Security*, vol. 15, no. 4, pp. 96–107, 2023.

Authors’ Profiles

Serhii Vladov is a Head of the Department of Scientific Work Organization and Gender Issues at Kremenchuk Flight College of Kharkiv National University of Internal Affairs. He is a Candidate in Technical Sciences. His current research and the fields of specialization – development of applied intelligent systems (including intelligent automatic control systems) of complex dynamic objects, in particular, helicopter turboshaft engines. He has nearly 200 scientific papers, among them more than 30, which are indexed in the Scopus scientific database.

Oleksandr Muzychuk is Doctor of Science, Professor, Vice-Rector of Kharkiv National University of Internal Affairs. Awarded with a Certificate of Honor from the Verkhovna Rada of Ukraine, as well as departmental commendations: the "For Distinction in Service" II degree badge, the "10 Years of the Ministry of Internal Affairs of Ukraine" medal, the "For Conscientious Service" III degree medal, the «For Distinction in Service» I degree badge, the «Honorary Badge of the Ministry of Internal Affairs», the «Best Employee of the Ministry of Internal Affairs» badge, and the "For the Safety of the People" badge. Published over 200 scientific and educational-methodological works, including 170 of a scientific-practical nature and 30 of an educational-methodological nature. Under his scientific supervision and guidance, 10 doctoral and 45 candidate dissertations have been defended.

Victoria Vysotska is Associate Professor at the Information Systems and Networks Department of Lviv Polytechnic National University. She defended her Doctoral degree in Technical Science, speciality in «structural, applied and mathematical linguistics» in 2023 on the topic "Analysis and synthesis of computational linguistic systems for processing Ukrainian textual content" Also, she received a PhD degree in Information Technologies from Lviv Polytechnic National University in 2014. She has currently published more than 500 publications. Her main research interests are focused on the identification of disinformation/fakes/propaganda, detection of sources of disinformation and inauthentic behaviour (bots) of coordinated groups based on artificial intelligence, NLP, computer linguistics, data science, system analysis, information technologies, machine learning, cyber security.

Alexey Yurko is an Associate Professor of the Department of Computer Engineering and Electronics, Kremenchuk Mykhailo Ostrohradskyi National University, Kremenchuk, Ukraine He is a Candidate of Technical Sciences. Research interests: electronic digital systems, computer modelling of processes and systems, transmission and signal coding. He has nearly 100 scientific papers.

Dmytro Uhryn graduated from Yuriy Fedkovych Chernivtsi National University, Chernivtsi. Currently, he is a Doctor of Technical Sciences and associate professor at Yuriy Fedkovych Chernivtsi National University. He has currently published more than 170 publications. His research interests are data mining, information technologies for decision support, swarm intelligence systems, and industry-specific geographic information systems. His areas of scientific interest are decision support information technologies, swarm intelligence systems and industry geoinformation systems.

How to cite this paper: Serhii Vladov, Oleksandr Muzychuk, Victoria Vysotska, Alexey Yurko, Dmytro Uhryn, "Modified Kalman Filter with Chebyshev Points Based on a Recurrent Neural Network for Automatic Control System Measuring Channels Diagnosing and Parring off Failures", International Journal of Image, Graphics and Signal Processing(IJIGSP), Vol.16, No.5, pp. 36-61, 2024. DOI:10.5815/ijigsp.2024.05.04